SLAC-PUB-948
(TH) and (EXP)
August 1971

ELECTROMAGNETIC INTERACTIONS WITH EMPHASIS ON COLLIDING RINGS, PARTONS, AND THE LIGHT CONE*

S. D. Drell

Stanford Linear Accelerator Center
Stanford University, Stanford, California 94305

Rapporteur's Report

The Amsterdam International Conference on Elementary Particles, Amsterdam, June 30 - July 6, 1971.

*Work supported by the U. S. Atomic Energy Commission.

I. INTRODUCTION

It is abundantly clear from the research results of the past few years that the study of particle physics via electron and photon scattering experiments plays an essential and unique role in the investigation of the structure of the hadrons. The importance of the electromagnetic interaction derives from three facts: (1) it is well understood, i.e., Maxwell and Dirac tell us all we need know. This a fact checked to the limit of precision in all experiments from 10^{-10} eV accuracies in the Lamb shift to QED interactions at several BeV interaction energies and momentum transfers; and from distances of several earth radii down 24 orders of magnitude to better than nucleon compton wave lengths or tenths of fermis;[1] (2) it is well treated in the formal analysis, i.e., the smallness of the fine structure constant allows expansion in powers of 1/137; and (3) it exhibits a local, point-like nature, i.e., the known electromagnetic field generated during the electron's scattering which interacts with the electromagnetic current of the hadron target can in fact probe the structure and properties of the target nucleon at arbitrarily small distances. To accomplish this one varies the photon size by tuning its mass or invariant momentum transfer to arbitrarily large values. This is in contrast to hadron-hadron scattering, in which the basic interaction between the target and beam particles is both unknown and diffuse.

The measurements of inelastic electron scattering performed at SLAC in the past few years have given evidence of a scale-invariant behavior of the proton and neutron structure functions which strongly hints at a rich substructure within the nucleon itself. These measurements suggest a very simple picture of the proton as a composite system built up of point-like constituents, just like the atom itself and the nucleus.

The key observation is the following: For elastic scattering from the proton, or inelastic scattering leading to a specific resonant state, the cross sections are observed to decrease roughly as $(1/Q^2)^4$ relative to their values for scattering from a point proton (with the observed magnetic moment):

$$\left(\frac{d\sigma}{d\Omega}\right)_{\text{exptl}} \simeq \left(\frac{d\sigma}{d\Omega}\right)_{\text{point}} \cdot \left(\frac{1}{Q^2}\right)^4 \quad \text{for } Q^2 \gtrsim \text{several GeV}^2 \tag{1}$$

i.e., the proton scatters as a diffuse composite system, just like an atom or a nucleus.

However, if one turns to very inelastic scattering in the continuum region as illustrated in Fig. 1, the cross section for inelastic scattering summed over all available hadron channels – i.e., the "inclusive" cross section – behaves as if the proton is built up of a number of hard chunks or pieces. To see this most simply, let us say there are $\frac{1}{x}$ chunks each of mass (xM) and charge xe). Assume for the moment that these chunks are loosely bound to one another so that if the proton is given a hard kick by the electron it breaks up with the scattering from each chunk being both elastic and incoherent: i.e., we can apply the impulse approximation to the scattering from individual chunks. The kinematic relation for elastic scattering from one of these chunks of mass (xM) is

$$Q^2 = 2(xM)\nu$$

and the cross section is given by

$$\frac{d\sigma}{d\Omega} = \left(\frac{d\sigma}{d\Omega}\right)_{\text{point}} \cdot \left(\frac{xe}{e}\right)^2 \cdot \left(\frac{1}{x}\right) \tag{2}$$

where the second factor is the square of the mean charge per chunk and the factor $\frac{1}{x}$ is just the number of chunks, each contributing incoherently of the

others, that make up the proton. More generally, not all chunks need have the same x but there may be a distribution $\rho_i(x)$, $\int_0^1 dx\rho_i(x) = 1$, of chunks of various types i with fractional charges $\lambda_i e$ so that (2) becomes (spin will be treated later)

$$\frac{d\sigma}{d\Omega} = \left(\frac{d\sigma}{d\Omega}\right)_{point} \sum_{i=1}^{N} \lambda_i^2 \rho_i(x)\,dx \equiv \left(\frac{d\sigma}{d\Omega}\right)_{point} \frac{dx}{x} \nu W_2 \qquad (3)$$

Missing from (2) and (3) is a form factor $F(Q^2)$ decreasing with large Q^2 as found in (1). Such a decreasing function of Q^2 would be present if the individual chunks were composite and their charges were distributed rather than point-like. The well known SLAC-MIT experiments[2] have confirmed that νW_2 is a function of x alone, independent of Q^2, a fact which I may remind you of in Fig. 2.

This is, of course, an absurd model for the proton or neutron. Whatever are its constituents – or partons as named by Feynman – they are presumably very tightly bound together by an energy at least comparable to and probably greater than their rest energies. Therefore a picture of chunks of point-like matter only weakly interacting makes little sense.[3] Nor can we identify the characteristics of these chunks by looking at the debris emerging from a proton after a high energy, very inelastic collision. Due to their strong binding, the constituents seen by instantaneous snapshots – i.e., in very inelastic scattering events – are undoubtedly very different in major and qualitative ways from the freely emerging debris.[4] However, as suggested by Feynman,[5] we may help our intuition and view the constituents as propagating in long lived, almost real and free states if we take advantage of the time dilation by boosting ourselves to a very rapidly moving reference frame – known to the theoretician as the infinite momentum or $P \to \infty$ momentum. Then if the momentum components of the

constituents were bounded in the rest frame, simple kinematics show that $x \equiv Q^2/2M\nu$ is just the fraction of the longitudinal momentum (as $P \to \infty$) on the particular parton from which the electron scatters elastically. In this reference frame and to those partons with finite $x = Q^2/2M\nu$ that are given a strong and sudden kick by the electron transferring high ν and Q^2, one can apply the impulse approximation. It is important to emphasize that the ratio x must be finite for this simple impulse picture. Otherwise, as illustrated in Fig. 3, we are forced to deal with very slow partons in the $P \to \infty$ system, or, as seen in the rest system of the proton, with the high momentum extremities of the bound-state structure, and for these the impulse approximation breaks down.[6]

II. COLLIDING RINGS

Enough for the introduction. Do we really know, or believe that there are point-like constituents inside the proton as there are electrons in an atom? In what sense is it correct to say that a proton, whose time average structure was revealed to be composite and extended by the elastic scattering measurements, is seen by the very inelastic scattering, or sudden snapshots, to be like a jam with seeds rather than like a jelly with none? Is this notion of constituents even a useful one or should we look more formally at the theoretical structure of the algebra of the commutators and products of local current operators near the light cone? To start trying to answer these questions we turn to the colliding ring experiments with their time-like photons.

What do we want to look for? First of all, if there are electrically charged point-like constituents, then within the framework of any local, relativistic theory we must pair produce them in the process

$$e\bar{e} \to ?\bar{?}$$

where ? denotes a parton. The ? will subsequently decay to observable final products but if we sum over all final hadronic states the cross section should depend on the colliding ring energy $s = q^2 = (2E)^2$ as $1/E^2$ which is the same energy dependence as for $e\bar{e}$ annihilation to point-like muon pairs:

$$\sigma_{e\bar{e}\to\mu\bar{\mu}} = \frac{4\pi\alpha^2}{3(2E)^2} \equiv \sigma_\ell \approx 21 \text{ nb}/E^2_{\text{GeV}} \quad . \tag{4}$$

In fact, the total annihilation cross section can be written

$$\left(\sigma_{e\bar{e}}\right)_{\text{hadrons}} = \frac{4\pi\alpha^2}{(2E)^2}\ \rho(4E^2)$$

$$\rho(q^2)(q_\mu q_\nu - g_{\mu\nu} q^2) = 4\pi^2 \sum_n (2\pi)^4 \delta^4(P_n - q)$$

$$\times \langle 0 | J_\mu | n \rangle \langle n | J_\nu | 0 \rangle$$

$$= 4\pi^2 \int d^4x e^{iq\cdot x} \langle 0 | \left[J_\mu(x),\ J_\nu(0) \right] | 0 \rangle$$

(5)

Using the free quark algebra for almost equal time current commutators – i. e., the free field algebra of currents made of bilinear products of fundamental spin $\frac{1}{2}$ quark fields,[7] we have:

$$\sigma = \sigma_\ell \left\{ \frac{4}{9} + \frac{1}{9} + \frac{1}{9} \right\} = \sigma_\ell \left\{ \frac{2}{3} \right\} \tag{6}$$

More generally the total cross section can be written as a sum over contributions from all types of partons, or elementary constituents:[8]

$$\sigma = \sigma_\ell \left\{ \sum_{\substack{J=1/2 \\ \text{partons}}} \lambda_J^2 + \frac{1}{4} \sum_{\substack{J=0 \\ \text{partons}}} \lambda_J^2 \right\} \tag{7}$$

Two questions of special interest for experiments to answer are:

(1) Does $\sigma \sim 1/E^2$ as suggestive of points constituents or does it it decrease more rapidly? Or even more slowly?

(2) Is the coefficient of σ_ℓ less than one, indicative of fractionally charged spin 1/2 objects as in (6) or is it greater than one: for example is it $1 + 1/4 = 5/4$ as in an SU_2 symmetric pion-nucleon theory, or $4 + 2/4 = 9/2$ as in an SU_3 theory of point meson-baryon constituents?

What do we know about this cross section?

New results were reported to this conference from Frascati and Novosibirsk and have greatly extended earlier published data. I will focus on the higher energy results $1.4 \text{ GeV} \leq 2E \leq 2.4 \text{ GeV}$. The "boson" group at Frascati[9] has more than tripled its total number of good events to 802. These involve at least 2 charged particles that are non-coplanar by at least 13° and do not shower like electrons or penetrate like muons. In three-fourths of the events observed just 2 charged non-coplanar tracks are observed. The background subtraction due to cosmic rays and beam-gas initiated tracks is very clear. However, the detector efficiency for multibody events of unknown angular distribution and multiplicity is dangerously uncertain when only 1/4 of the 4π solid angle is covered. Assuming isotropic production, the boson group has presented the results in Fig. 4 which leads to a total cross section averaged over the full energy interval of

$$\sigma_{e\bar{e} \rightarrow \text{hadrons}} \approx 30 \pm 10 \text{ nb} \tag{8}$$

The energy dependence is not incompatible with an $1/E^2$ fall off as in (4) and the magnitude is also comparable with the point muon cross section in (4).

In another Frascati experiment reported to the conference by the γ-γ group[10] the detectors include large blocks of scintillation counters as well as spark chambers and the criterion for an event includes seeing at least three "particles" – i.e., charged particles or photons since the γ-ray detection efficiency is very high in this setup. The total cross section in this case, with 70% of the events being collected for a total colliding beam energy in the neighborhood of 2 BeV, is

$$\sigma_{e\bar{e}\to\text{hadrons}} = 15 \pm 6 \text{ nb} \qquad 1850 \text{ GeV} \leq 2E \leq 2100 \text{ GeV} \tag{9}$$

which is consistent with (8). The comparison with (8) is especially favorable if the cross sections are in fact decreasing as $1/E^2$. In this experiment two-thirds of the events are of the type with two charged particles plus neutrals, and the remaining correspond to at least four charged tracks.

These observations are reminiscent of the point-like constituent features of deep inelastic scattering: large cross sections, point-like in magnitude and with an energy variation consistent with a $1/E^2$ fall off.

It will be important to have an accurate determination of the energy dependence of this cross section – and in particular it is important to learn at what energy range, if any, we are beyond resonance structures entirely and can speak of a smooth asymptotic energy dependence.

At slightly lower energies between 1180 MeV and 1340 MeV for the total collision energy, Novosibirsk[11] has also observed multimeson events. The solid angle of their detectors is about a factor of 2 smaller than at Frascati and assuming an isotropic distribution of four particles for the production mechanism in order to calculate a detection efficiency they come out with a cross section estimate of

$$\sigma = 100 \pm 30 \text{ nb} \quad . \tag{10}$$

Theoretical studies carried out over the past year or so suggest that a sizable fraction of the observed cross section can be attributed to processes such as illustrated in Fig. 5. Indeed the calculations of Layssac and Renard[12] submitted to this conference along with earlier ones of Renard[13] and Kramer, Uretsky and Walsh[14] suggest that even at 2 GeV enough decay modes of the ρ, ω and ϕ mesons are opening up that they can account for upwards of 10 nb of cross section by the vector decay chain of a virtual ρ, ω, ϕ decaying to a resonance $R = (A_1, A_2, B, \rho, \omega)$ plus either a π, K, or another resonance, followed by subsequent decay of the resonances themselves. It is suggested that the rapid decrease in vector meson production as we go above the ρ, ω, ϕ masses and into the tails of their production curves is offset by two effects: (a) the crossing of new production thresholds and (b) growing decay matrix elements as calculated on the basis of elementary point coupling models with the coupling coefficients determined by the vector dominance model, experimental branching ratios, and SU_3. Although crude in nature, these estimates are important because of their large size. Yet another important factor may defer the on-set of high energy limiting behavior for time-like electromagnetic amplitudes. If there are particles on many linearly rising trajectories a la Veneziano, additional vector mesons will couple to the photon in Fig. 5 and may lead to a very different energy variation. The possible ρ' at 1.5 ± 1 GeV is one such candidate.[15]

Proceeding further one can study the reaction

$$e\bar{e} \rightarrow h + \text{anything} \qquad (11)$$

as a function of the energy deposited on the one detected hadron h. The kinematic region being probed by such processes is shown in Fig. 6. Once again we should

observe a scaling law

$$\frac{d^2\sigma}{dw\, d\cos\theta} = \frac{\pi\alpha^2}{3E^2}\left[\mathscr{F}_1(w) + \mathscr{F}_2(w)\,\sin^2\theta\right] \tag{12}$$

where $0 < w \equiv \frac{2P\cdot q}{q^2} < 1$ is twice the fraction of the total $e\bar{e}$ energy appearing on the detected hadron in the colliding ring frame and is the analogue of x in (2) and (3); θ is the angle between the detected hadron and the collision axis.

There are three questions of special interest for the experiments to answer here[16]:

(1) Does $d\sigma/dw$ scale as $(1/E^2)\ \mathscr{F}(w)$?

(2) How do the magnitude and w dependence of $\mathscr{F}(w)$ in (12) compare with the analogous deep inelastic structure function?

(3) How accurate are predictions of invariance principles at high energies such as C invariance of hadronic electromagnetic interactions[17] and SU_3 symmetry together with the hypothesis that the electromagnetic current is a U-spin singlet?[16]

If the hadronic states are further restricted by exclusive measurements we might expect to find that individual channels are produced with small cross sections that are reduced by decreasing form factors at higher energies, analogously to the observed scattering results. Thus, two-body final states such as

$$e\bar{e} \to p\bar{p} \tag{13}$$

$$ee \to \pi^-\pi^+ \tag{14}$$

would be produced with form factors as in (1) that reduce the cross sections below the point-like result of (4) and are small for large s. The applicable formulas are

$$\sigma_{e\bar{e}\to\pi^-\pi^+} = \frac{\pi\alpha^2}{12E^2}\,\beta_\pi^3\,\left|F_\pi(s)\right|^2 \quad ; \quad s = 4E^2 \equiv q^2 \tag{15}$$

$$\sigma_{e\bar{e}\to p\bar{p}} = \frac{\pi\alpha^2}{3E^2}\,\beta_p\left\{\left|G_M(s)\right|^2 + \frac{M^2}{2E^2}\left|G_E(s)\right|^2\right\} \tag{16}$$

The pion form factor was measured in and near the ρ - ω resonance region both at Orsay and Novosibirsk and its interpretation along with ρ, ω mixing and the leptonic decay rates were thoroughly and clearly discussed last fall in the Balaton Symposium by Professor Sakurai.[18] I have nothing to add to the general picture of a good qualitative and improving quantitative fit. When we move to higher energies we want to learn whether $F_\pi(s)$ falls as a simple ρ-dominant expression as $F_\pi \sim \frac{1}{1-s/M_\rho^2}$ for $s \gtrsim 2$ GeV^2 or whether there are additional peaks, such as the ρ itself where $\left|F_\pi(s)\right|^2 \sim 50$, or valleys. No new results were reported here on these measurements but recall that[18] at $s = 3$ GeV^2, the Frascati results indicate $\left|F_\pi(s)\right|^2 \sim 1/2 - 1/3$ whereas $\left|\frac{1}{1-s/M_\rho^2}\right|^2 \sim 1/20$. What this long tail is due to – theoretically or experimentally – still remains to be settled. In fact, so does the entire question of whether $F_\pi(s)$ decreases for large space or time-like values of s as $1/s^2$ as observed for proton form factors in electron scattering experiments at large s. Bjorken[19] suggests that $F_\pi(s)$ should fall as $1/s$, not $1/s^2$, based on the following pictorial mnemonic: The quark or parton is point-like; the nucleon with 3 quarks decreases as $1/s^2$; so the pion as a quark pair may be decreasing only as $1/s$. (See Fig. 7.)

There are other suggestions, both theoretical and experimental, that the pion radius should be closer to a ρ-dominant value of $-\langle R^2 \rangle = 6/M_\rho^2$ than found for the proton.[20]

For the proton structure the preliminary new results from Frascati[21] as reported to this conference are that at $E = 1.05$ GeV

$$\sigma_{e\bar{e}\to p\bar{p}} = 10^{-32}\ \text{cm}^2 \left\{ \left|G_M(4.4)\right|^2 + \frac{M^2}{2.2\ \text{GeV}^2} \left|G_E(4.4)\right|^2 \right\}$$

$$\leq 0.94 \times 10^{-33}\ \text{cm}^2 \qquad \text{(2 standard deviations)} \tag{17}$$

These numbers are based on 8 ± 4 candidate events after background subtraction. The upper limit of (17) corresponds to 16 real events. This sample of machine induced good events is defined by the requirements of collinearity to better than 16^{o}, identification of one particle as a stopping proton and of the oppositely directed one as heavily ionizing. Further analysis is in progress on the energy deposition of the latter. The significance of this result as related to earlier $p\bar{p}$ annihilation work[22] is illustrated in the next two figures (Figs. 8 and 9). A rapidly dropping form factor here is of course consistent with the concept of point-like constituents in the proton just as it is for elastic scattering. If these constituents are free to escape, the probability of a proton remaining in one piece, will be very small after it receives a hard blow.

I have dwelt at length on colliding ring physics which, though still in its labored infancy, is opening our eyes to an entire new time-like world because:

(1) I believe this is a tremendously exciting first vision of this new world.

(2) The union of results from massive time-like as well as space-like electromagnetic currents (perhaps weak ones also) will be decisive in answering whether there are, and what and how many are, seeds in a nucleon; and

(3) We must now turn to a very practical issue – usually called a radiative correction – which has to be better understood on a quantitative level before we can know what is really going on. These considerations, most thoroughly appreciated and analyzed by a number of groups in the last year, will have major impact on how the detection equipment for colliding ring physics should develop.

The important radiative correction is given by the amplitude for 2-photon annihilation by the process

$$e + e^{\pm} \rightarrow e + \gamma^* + e^{\pm} + \gamma^* \rightarrow e + e^{\pm} + X \qquad (18)$$

as illustrated in Fig. 10. Although this process is of order α^4, whereas the familiar lowest order one photon contribution is of order α^2, two factors operate to overcome this added factor of α^2 and to promote it to importance[23]:

(1) We expect the cross section for the one photon process to decrease at high energies as $1/s \sim 1/E^2$ even for point-like constituent theories as in (4), (6), and (7). In contrast, the "almost real" photons radiated by the electrons favor large impact parameter collisions and the cross section will vary as a constant $1/M_x^2$ where M_x is commonly the threshold mass of the state formed in the photon-photon annihilation.

(2) We also expect the cross section to be enhanced by familiar logarithmic factors of the form $\ell n\, E/m_e$, one for each of the electron lines, and these are sizable (~7.5 for E = 1 BeV). Additional logarithms as inferred from the Cheng-Wu analysis[24] of massive electrodynamics are also expected depending on the high energy behavior of the $\gamma\gamma$ annihilation process.

This is a very practical example of the general phenomena discussed by Cheng and Wu[25] in which the asymptotic behavior of higher order terms may be entirely different and indeed of controlling importance relative to the lower order ones. Beyond the two-photon intermediate state we expect to acquire more powers of α and logarithms but no more energy factors from three or more photons.[26]

In the equivalent photon approximation one can write a simple and intuitive expression for the total cross section to produce X by two oppositely directed photons of energies k_1 and k_2[23]:

$$d\sigma_{ee\to eeX}(E) \cong \int^{E} \left\{ \frac{dk_1}{k_1} \frac{2\alpha}{\pi} \frac{\left[E^2 + (E-k_1)^2\right]}{2E^2} \ell n \frac{E}{m_e} \right\} \cdot \left\{ \frac{dk_2}{k_2} \frac{2\alpha}{\pi} \frac{\left[E^2 + (E-k_2)^2\right]}{2E^2} \ell n \frac{E}{m_e} \right\} d\sigma_{\gamma\gamma\to X}(k_1, k_2) \tag{19}$$

where the expressions in brackets represent the Weiszacker-Williams, or equivalent photon, spectrum of an electron of energy E; and $d\sigma_{\gamma\gamma\to X}(k_1, k_2)$ is the differential cross section for the two colliding "almost real" photons to produce a given final state X. The final electrons are not detected. For the total cross section to produce a given final state of any mass this integrates to

$$\sigma_{ee\to eeX}(E) \cong 2\left(\frac{\alpha}{\pi}\right)^2 \ell n^2\left(\frac{E}{m_e}\right)\int_0^{4E^2} \frac{ds}{s}\, \mathcal{F}\left(\frac{\sqrt{s}}{2E}\right) \sigma_{\gamma\gamma\to X}(s)$$

where (20)

$$\mathcal{F}(x) = (2 + x^2)^2 \ell n \frac{1}{x} - (1 - x^2)(3 + x^2)$$

What is the significance of this result? This is best seen by looking at Fig. 11 from the paper of Brodsky et al.,[23] which compares the $\pi^{\pm}$-pair production cross section, assuming point pions in the one and two-photon processes (14) and (18) where $X \equiv \pi^+\pi^-$. In this case (18) becomes for very large E/m_e

$$\sigma_{ee\to ee\,\pi^+\pi^-}(E) \cong \frac{16\alpha^4}{9\pi} \frac{1}{m_\pi^2}\left(\ell n^2 \frac{E}{m_e}\right)\left(\ell n \frac{E}{m_\pi}\right)$$

$$\cong \left\{\frac{64\alpha^2}{3\pi^2} \frac{E^2}{m_\pi^2}\, \ell n^2 \frac{E}{m_e}\, \ell n \frac{E}{m_\pi}\right\} \sigma_{e\bar{e}\to\pi^+\pi^-}(E) \qquad (21)$$

where we have used (15) for point pions in writing the second line. Evidently the two photon cross section is very important. Of course pions are not point charges and there are structure corrections. An estimate of these in terms of a σ resonance is shown in Fig. 11 and further increases the 2γ contribution. In the total cross section (21) the σ shows its presence only as a quantitative effective on the cross section but there are no clear bumps to identify. In particular the region near the production threshold for $\gamma\gamma \to 2\pi$ is seen to be important in (20); and near threshold this cross section is relatively well known

since it is controlled by the Thomson limit as $m_\pi \to 0$. To use the colliding ring for detailed studies of the C = + resonances one has to make measurements that are differential in the electron's energies as in (19).

As long as the two γ process is studied in the equivalent photon approximation as in (19) and (20), the two pions will be coplanar with the $e\bar{e}$ collision axis. They are also predominantly produced along the colliding beam direction. In contrast with the one photon annihilation in which the two pions must be exactly back to back, they will have a strong tendency to come out with a narrow opening angle and hence be strongly noncollinear. This is because the two final pions will prefer parallel final directions in order to decrease the mass of their final state and take advantage of the low s weighting in (20).

Detailed theoretical studies of these features have been carried through this year stimulated by the exciting new experimental progress with colliding $e\bar{e}$ rings. To be quantitative about this contribution it is necessary to go beyond the leading logarithms in $\ell n(E/m_e)$ in the Weiszacker-Williams method that are retained in (20) and (21). One should use the complete expression for the equivalent photon spectrum, as done in the calculations for Fig. 11, both to calculate the magnitude of the total cross section to better than a factor of two for collisions in the few GeV range, as well as to calculate noncoplanarity effects in pair production processes such as

$$e\bar{e} \to e\bar{e}\,\pi^+\pi^- \quad .$$

Since the experiments on multiparticle hadron states use as an identification criterion the noncoplanarity of two observed charged particle tracks, it is important to understand the significance of this noncoplanarity effect which is defined in terms of the angle ψ between the two planes determined by each of the two outgoing pions and the $e\bar{e}$ collision axis as shown in Fig. 12. From their calculations

Brodsky et al. [23] find that the differential cross sections decrease typically only as $\left(\frac{d\psi}{\psi}\right)$ for large $\psi \gtrsim \sqrt{m_e/E}$ and that for example 50% of all pion pairs produced in the process $e\bar{e} \to e\bar{e}\,\pi^+\pi^-$ are emitted with a coplanarity angle $\psi > 13^o$ at Frascati energies. This is a large fraction of these 2γ events and our problem is to make certain that at the operating conditions of present as well as of planned and future colliding rings we can identify whether we are observing the 1γ or the 2γ process.

What can we say about the role of the 2γ process in present experiments? First of all, from a purely experimental point of view, the 2γ contribution has a very characteristic angular distribution that peaks for small coplanarity angles ψ and strongly emphasizes small angles between the produced hadrons and the colliding beam axis in order to form low mass final hadron states. No such peaking in ψ was observed by the Frascati "boson" group[9] in their analysis of the coplanarity distribution which is consistent with the 1γ annihilation process. The "$\gamma\gamma$" group[10] on the other hand has now managed to specifically identify such events by adding to their detectors two counters upstream and downstream of Adone's bending magnets which then serve as momentum analyzers. Their preliminary analysis is continuing. At Novosibirsk[11] the electron double pair production process $e\bar{e} \to (e\bar{e}) + (e\bar{e})$ has been studied in detail at a total collision energy of 1020 MeV and the results for the cross section and azimuthal distributions agree well with Baier and Fadin's calculations[23] thus confirming the 2γ process for electrodynamic channels.

From a theoretical point of view the 2γ effect is expected to be a background correction rather than the dominant contributor at present energies and for nonforward solid angles for the detected hadrons. One is here talking of a cross section of a few nanobarns at most relative to measured cross sections

that are an order of magnitude larger. However, the importance of this contribution grows logarithmically with energy while the 1γ annihilation channels presumably decreas as $1/E^2$ as we noted earlier. Also the processes $e\bar{e} \to e\bar{e}\ \mu\bar{\mu}$ and $e\bar{e} \to 2(e\bar{e})$ continue to grow and are very much larger[27] due to their lower thresholds in (20) and (21). Therefore, rejection criteria for identifying muons (no nuclear interactions) and electrons (no showers) must be very good.

In order to remove all such 2γ processes from their position of prominance – or nuisance – if desired, all that is required is to verify that there are no electrons in the final state, or to insist that the mass of the final hadronic state is large. If a minimum mass of S_{min} is determined, (20) and (21) become roughly

$$\sigma(E;\, S_{min}) \sim \frac{\alpha^4}{\pi} \quad \frac{1}{S_{min}} \left(\ell n^2 \frac{E}{m_e} \right) \tag{22}$$

where numerical factors and additional logarithmic factors $\ell n\, E/\sqrt{S_{min}}$ are of ~ 1 and are not included. In terms of the two energies of the virtual photons, k_1 and k_2, explicitly appearing in (19), the mass of the hadronic state is given by

$$(k_1 + k_2)_\mu (k_1 + k_2)^\mu = 4 k_1 k_2 = s$$

and so the threshold condition can also be placed as a lower limit on the energy decrease of the electrons

$$4k_1k_2 > S_{min} \quad . \tag{23}$$

Any technique that puts a lower limit on the momentum detected on the hadrons or momentum loss by the colliding electrons will suffice to ensure a large enough S_{min} so that the two photon contribution can be reduced to a negligible contribution

relative to the one photon cross section. A rough criterion for this (apparent from (21) with m_π^2 replaced by S_{min} as in (22)) is that

$$\left(\frac{\alpha^2}{4\pi}\,\ell n^2\, E/m_e\right)\left(E^2/S_{min}\right) < 1 \tag{24}$$

This condition also puts an upper limit on how far one can push to measure the 2γ cross section at high energies as objects of interest in their own right.

Colliding rings have opened a beautiful and exciting field that is still in its infancy – a statement equally applicable to the CERN ISR for pp collisions as for the electron rings. Not only is its potential great, it has already come very far as the Orsay group reminded us at the conference[28] with its beautiful new results on ω production and decay, which can be summarized as follows:

ω production cross section	$\sigma_{res}(e\bar{e} \to \pi^+\pi^-\pi^o) = 1.70 \pm 15\ \mu b$
ω width	$\Gamma_{\omega \to} = (9.7 \pm 1.0)$ MeV
branching width	$\Gamma_{\omega \to e\bar{e}} = (.77 \pm .08)$ keV
branching ratio	$B_{\omega \to e\bar{e}} = (.79 \pm .08) \times 10^{-4}$

Before moving on, let me apologize explicitly to all whose work I am passing over – it is no reflection of lack of interest in or admiration of your contributions. It is only that my talk can last no more than one microcentury[29] and I want to stay with my theme of "are there point-like constituents in the proton, or is the proton more like a jelly or raspberry jam with seeds in it?"

III. PARTONS AND THE LIGHT CONE

At the beginning of the last section we asked whether there really were point-like constituents inside the proton; and we turned to the massive time-like photons or currents in $e\bar{e}$ collision for evidence and theoretical predictions of energy variations and scaling laws.

We would also like to confront these ideas of partons in the proton with additional tests. How do we identify new opportunities to do this, theoretically as well as experimentally?

Theoretically we can follow either of two lines of approach – the one more intuitive and embracing the notions of the impulse approximation in an appropriate $P \to \infty$ frame as I have described in the beginning of this report for deep inelastic electron scattering. The second one is more formal and is based on the analysis of the singular behavior of products and commutators of currents for light-like separations along the light cone. These are not just alternative languages for studying the same processes but have different regions of applicability.

They both apply for deep inelastic scattering when the mathematical object being probed is

$$W_{\mu\nu} = 4\pi^2 \frac{E_P}{M} \int d^4x\, e^{iq\cdot x} \langle P | \left[J_\mu(x),\ J_\nu(0) \right] | P \rangle$$

$$= -\left(g_{\mu\nu} - \frac{q_\mu q_\nu}{q^2} \right) W_1(q^2, \nu) + \frac{1}{M^2} \left(P_\mu - \frac{P\cdot q}{q^2} q_\mu \right) \left(P_\nu - \frac{P\cdot q}{q^2} q_\nu \right) W_2(q^2, \nu) \tag{25}$$

In the laboratory frame with

$$P^\mu = (M, 0, 0, 0) \qquad \omega \equiv 2M\nu / Q^2$$
$$q^\mu \cong (\nu, 0, 0, \nu + M/\omega) \tag{26}$$

the exponential is

$$e^{iq\cdot x} \cong e^{i\nu(t-z) - i(M/\omega)z} \tag{27}$$

If we assume that the matrix element has no high frequency oscillations to cancel the exponential (27) for $\nu \to \infty$ and $\omega > 1$ finite, then the important

space-time interval contributing to (25) will be

$$t - z \lesssim \frac{1}{\nu} \to 0$$
$$t,\ z \lesssim \frac{\omega}{M} \quad , \quad \text{i.e., finite} \tag{28}$$

and by causality in the commutators

$$0 \le x_\mu x^\mu \le \frac{2\omega}{M\nu} - x_\perp^2$$

or

$$x_\perp^2 \le \frac{4}{Q^2} \tag{29}$$

This region is shown in Fig. 13 and is a segment of finite length but of asymptotically vanishing invariant width about the light cone. The matrix element multiplying the exponent in (25) is a function of scalar variables $x_\mu x^\mu \sim 0$ and $x\cdot P = Mt \sim \omega$ that extend over a bounded range only. We are thus led to expand the matrix element about the light cone $x_\mu x^\mu \to 0$, identifying its light cone singularity by computing the light cone behavior from free field theory commutators along the light cone. The remaining dependence of the matrix element is governed by its $\omega = 2M\nu/Q^2$ variation. In this way the original scaling result predicted by Bjorken is reconstructed,[30] i.e.,

$$\nu W_2 = F_2\left(\frac{2M\nu}{q^2}\right)$$
$$MW_1 = F_1\left(\frac{2M\nu}{q^2}\right) \qquad \text{for } M\nu,\ Q^2 \gg M^2;\quad \omega \text{ finite} \tag{30}$$

As we saw in (2) and (3) the parton model leads to the same scaling behavior. In particular we can write (25) in the parton model and in terms of its space coordinates

$$W_\mu^\mu \sim \int d^4x e^{iq\cdot x}\, \square\left\{\Delta_+(x^2, M_P^2) \int_0^1 d\eta\, \eta \sum_i \lambda_i^2\ \rho_i(\eta)\ e^{iP_\eta \cdot x}\right\} \tag{31}$$

where λ_i is the parton charge in units of e and ρ_i is the momentum distribution of partons as in (3). This expression as constructed and analyzed by R. Jaffe[31] explicitly reveals the role of the light cone singularity in the matrix element. The positive frequency invariant singular function $\Delta_+(x^2, M_P^2)$ can be expanded around $x^2 \sim 0$ because of the high frequency oscillations in $e^{iq\cdot x}$ as shown in Fig. 13. There are no other high frequency oscillations in (31) to cancel this behavior since the integral over the parton distribution is well behaved and oscillates with the four momentum of the parton of mass M_P and with momentum fraction η

$$\left(P_\eta\right)^\mu \left(P_\eta\right)_\mu = M_P^2 \ll Q^2 \qquad \text{in the Bjorken limit.} \tag{32}$$

This amplitude can thus be approached either with the light cone algebra or the impulse approximation intuitive ideas of the parton model for deducing its scaling properties. The success of scaling can be linked in this case to our having the correct algebra of local current operators very near the light cone and with no specific recourse to notions of point-like constituents or partons. In order to further test the idea of partons we need to find a measurable process that meets the requirement of the parton model – i.e., we can apply the impulse approximation in an infinite momentum frame because the interaction delivers a hard, sudden kick to almost free constituents – but which does not get its contributions from the region near the light cone.

As an example which can be analyzed in terms of partons but not, I believe, in terms of the singularity structure near the light cone, I want to turn next to a process that has been observed by Cristenson et al., at Brookhaven[32] and is also a natural for the CERN ISR. This is production of massive lepton pairs in hadronic collisions – viz.

$$P + P \rightarrow (\mu\bar{\mu}) + \text{anything} \tag{33}$$

where the invariant (mass)^2 of the muon pair, Q^2, is large and a finite fraction of the collision total (energy)^2, $s = (P_1 + P_2)^2$, and so is the total hadronic mass in the final state. The total cross section for a given pair mass Q^2 is

$$\frac{d\sigma}{dQ^2} = \frac{4\pi\alpha^2}{3Q^2 s} \; W(Q^2, s);$$

$$W(Q^2, s) = -16\pi^2 E_1 E_2 \int_{q_0>0} d^4q \, \delta(q^2 - Q^2) \int d^4x e^{-iq\cdot x} < P_1 P_2^{in} \left| J_\mu(x) J^\mu(0) \right| P_1 P_2^{in} > . \tag{34}$$

Whereas the colliding ring total cross section led us to consider the vacuum expectation value of the current commutator in (5), and deep inelastic scattering probed the one particle matrix element of the current commutator in (25), we now face the two-particle matrix element of a product of currents, not their commutator, in (34). The same arguments used for confining ourselves to a small strip along the light cone in (28) and (29) and Fig. 13, lead us right down to the tip of the light cone in (5) as $q_0 = 2E \to \infty$ and $t \sim \frac{1}{q_0} \to 0$; $\vec{x}^2 < t^2 \to 0$. The asymptotic behavior of (5) is often expressed in terms of equal time commutators of the currents, and if ∞ Schwinger terms are present lead to a $1/s \sim 1/E^2$ behavior for $(\sigma_{e\bar{e}})_{hadrons}$ in (5).

In (34), however, we face a new situation. In contrast to the deep inelastic scattering where we could approach the light cone by taking the limit $\nu \to \infty$ in the laboratory frame with a fixed nucleon at rest as in (26), we here must deal with the limiting process

$$\begin{aligned} &Q \to \infty \text{ and } s \to \infty \text{ so that} \\ &Q^2/s < 1 \text{ and finite} \end{aligned} \tag{35}$$

where s is the total invariant mass of the colliding 2-nucleon system; this is the experimentally accessible region. This dual limiting procedure introduces arbitrarily high frequency components into the matrix element in (34) which will be arbitrarily ignored if we simply expand the 2-nucleon matrix element about the light cone and retain only the leading singularity in the product of currents for a light-like separation $x^2 \to 0$. Justification of such an expansion can only come from detailed dynamical assumptions[33] of high energy limits for the matrix element (6 point function) in (34).

The simplest intuitive picture of the elementary interaction leading to production of a massive pair in (33) is as illustrated in Fig. 14. As viewed in the collision center-of-mass a right moving parton associated with P_1 and with momentum $\eta_1 P$ annihilates on a left moving antiparton associated with P_2 and with momentum $-\eta_2 P$. Since their energies add while their oppositely directed momenta subtract they form a massive pair state with

$$Q^2 \approx \left[(\eta_1 + \eta_2)P\right]^2 - \left[(\eta_1 - \eta_2)P\right]^2 = 4\,\eta_1\,\eta_2 P^2 \cong \eta_1\,\eta_2 s\,. \tag{36}$$

This mechanism allows almost real constituents of the proton with finite momentum fractions η_1 and η_2 to annihilate suddenly and to form the observed final state. Intuitively it leads directly to a cross section, which can also be derived[34] by identical methods leading to scaling for (3) and (12),

$$\frac{d\sigma}{dQ^2} = \frac{4\pi\alpha^2}{3Q^2} \int_0^1 d\eta_1 \int_0^1 d\eta_2\, \delta(Q^2 - \eta_1\,\eta_2 s) \sum_i \lambda_i^2\, \rho_i(\eta_1)\bar{\rho}_i(\eta_2) \tag{37}$$

where $\rho_i(\eta_1)$ and $\bar{\rho}_i(\eta_2)$ are respectively the probabilities for finding a parton and antiparton of type i with momentum fractions η_1 and η_2 as related through

(36). The densities ρ_i are related to deep inelastic structure functions, as shown in (3), and so we have established a connection between this and the deep inelastic scattering cross sections that is expressed by

$$\frac{d\sigma}{dQ^2} = \frac{4\pi\alpha^2}{3(Q^2)^2}\int_0^1 d\eta_1 \int_0^1 d\eta_2\, \delta\left(\eta_1\eta_2 - \frac{Q^2}{s}\right)\sum_i \frac{1}{\lambda_i^2}\left[\overline{\nu W_2}(\eta_1)\right]_i \left[\nu W_2(\eta_2)\right]_i$$

$$\propto (1/Q^2)^2 \quad \mathcal{F}(Q^2/s) \tag{38}$$

In particular Eq. (38) gives a scaling law in addition to a quantitative relation to deep inelastic scattering. The scaling law can be derived on more general assumptions[34] than required for the specific expression (38) in terms of factored structure functions for the two incident protons. It will be important to test.

I'll return shortly to the attempts to fit (3) and (38) simultaneously to experiment, but first I want to analyze what role the light cone plays in (37) and (38). In order to investigate this Jaffe[31] has recast these parton expressions in terms of space-time coordinates, by constructing the following identity:

$$\delta(Q^2 - \eta_1\eta_2 s) = \int_{q_0>0} d^4q\, \delta(q^2-Q^2)\int \frac{d^4x}{(2\pi)^4}\, e^{-iq\cdot x}\left[e^{iP_{\eta_1}\cdot x}\right]\left[e^{iP_{\eta_2}\cdot x}\right] \tag{39}$$

where P_{η_1} and P_{η_2} are the four momenta of the right and left moving (anti)-parton with space momenta $\eta_1\vec{P}$ and $-\eta_2\vec{P}$, respectively. Equation (37) now reads

$$\frac{d\sigma}{dQ^2} = \frac{4\pi\alpha^2}{3Q^2}\int_{q_0>0} d^4q\, \delta(q^2-Q^2)\int d^4x\, e^{-iq\cdot x}\cdot \tag{40}$$

$$\cdot\left\{\sum_i \lambda_i^2 \int_0^1 d\eta_1 \rho_i(\eta_1)\, e^{iP_{\eta_1}\cdot x}\int_0^1 d\eta_2\, \bar{\rho}(\eta_2)\, e^{iP_{\eta_2}\cdot x}\right\}$$

and we see in (40) that the two nucleon matrix element of the product of current operators appearing in (34) has not introduced a light cone singularity but only very high frequency oscillations. In fact, the parton model has picked out the nonsingular part of the product of the current operators in the mechanism of annihilating the parton pair. In contrast to a parton propagator as in (31), (40) contains a propagator for the virtual photon that produces the lepton pair. This is the system that propagates into the final state, and the propagator is displayed by doing the integral

$$\int_{q_0>0} d^4q \ \delta(q^2 - Q^2) \ e^{-iq\cdot x} \propto \Delta_+(x^2, Q^2) \ .$$

This propagator is introduced by the final state kinematical integrals, however, and does not come from the structure or algebra of the current matrix element.

The product of exponentials of the oppositely directed momentum vectors of the pair in (40) has the high Fourier frequencies to carry the integrand away from the light cone in contrast to (31). Rather than the light cone, it is the mass shell that plays the dominant role. Specifically, the scaling law (38) emerges when the intermediate propagators are near their mass shells (or "long lived") in Feynman amplitudes, such as Fig. 15.

Equation (38) is an example of a scaling law that emerges from a parton model but not from a light cone analysis. Contributions to the cross section come from all of the space-time intervals between the two current operators in (34). In this the massive lepton pair production experiment differs from deep inelastic electron scattering in an important way. Experimental testing of the scaling prediction (38) is of great importance and will contribute to our appreciation of the role of the light cone in these processes. The notion of "point-like constituents

in the nucleon" will be much more compelling, I believe, if the scaling law (38) is established experimentally. It cannot be directly attributed to light cone behavior alone.

Another example of a measurable process that can be analyzed in the parton but not light cone language is deep inelastic photoproduction of massive lepton pairs:

$$\gamma + p \rightarrow \mu\bar{\mu} + \text{anything} \tag{41}$$

In this case, what is measured is a product of the parton distributions of the photon and the proton, as illustrated in Fig. 16. Jaffe[35] has made a detailed study of this process also and established the conditions for separating the parton contribution from the normal Bethe-Heitler production which has a very large "elastic" peak when the photon transfers all or almost all of its energy to the muon pair. Figure 17 shows a typical prediction appropriate to DESY. Confirmation of an excess over the Bethe-Heitler prediction and observation of the scaling behavior will be of great interest in beginning to probe the hadronic constituent structure of a real photon.

Another way of probing the photon structure is by deep inelastic scattering of electrons in ee colliding ring collisions.[36] In this case the deep inelastic scattering takes place from the virtual, almost real, photon spectrum of the "target electron":

$$e + \gamma\,(\text{real}) \rightarrow e' + \text{anything} \quad . \tag{42}$$

The projectile electron is kinematically constrained to deliver large q^2 and ν as in the SLAC experiments. The recoil of the target electron with known momentum and at small angles is also detected so that the almost real target photon has a known frequency and the conditions for Bjorken scaling are satisfied,

as shown in Fig. 18. If this process can be measured with high luminosity rings and scaling verified, it will provide a direct measurement of the photon's parton structure. Cross sections as large as $\sim 10^{-34}$ cm^2/GeV are estimated for E = 2.5 GeV, $\nu > 1.5$ GeV^2, and $Q^2 = .17$ GeV^2, which exceeds the few pion threshold and may be appropriate for the scaling region. Process (42) differs from (41) in that it provides us with an opportunity to probe the photon near the light cone, in contrast to (41), but in analogy with deep inelastic scattering which also probes the proton also near the light cone, as we have discussed in Fig. 13.

There has also been much recent theoretical progress in studying[37] physical amplitudes that emphasize the light cone region but do not lie within a conservative parton framework that is based on the application of the impulse approximation to almost real, long lived, partons propagating near to their mass shells and scattering independently of each other.

The relation between the parton and light cone analysis is not totally clear at this time. The goal of understanding this relation will undoubtedly inspire much work and progress in the year ahead.

IV. MODELS FOR FITTING THE DATA

For the final part of this report I want to return to the SLAC-MIT deep inelastic scattering data and discuss some general aspects of the models, parton pictures, data fits, and predictions it has inspired as well as the questions it has raised.

Conceptually the most direct approach is simply to accept the observed fact that scaling has set in already at relatively low values of $Q^2 \gtrsim 1$ GeV^2 and $\nu \geq 2$ GeV in terms of the modified scaling variable of Bloom and Gilman[38]

$$\omega' \equiv \omega + M^2/Q^2 \equiv 1/x'$$

The parton model treating the proton and neutron as built of point-like incoherently and independently scattering constituents is then applied. This approach, which has been widely applied, was most completely developed in the spirit of a quark model in a recent paper by Kuti and Weisskopf.[39] It is instructive to see how far one can get with experimental fits and predictions with the simple view of partons as quarks.

Kuti and Weisskopf build the nucleon in an infinite momentum frame with a wave function constructed as a product of three parts: the three valence quarks that give the nucleon its unitary spin as well as spin quantum numbers and are responsible for the nondiffractive contribution to the scattering as observed in the difference between neutron and proton deep inelastic scattering; a "sea" or "core" of quark-antiquark pairs assumed to form singlet states; and a "glue" of neutral constituents that are thought to give rise to the forces holding the valence quarks and the sea together. Both the sea and glue are needed in fitting the observed shape of νW_2 as a function of x' as well as the neutron-proton difference.

The sea and glue partons are given a dx/x spectrum in order to account for the observed constancy of νW_2 as $x \to 0$ (see Eq. (3)) which is also correlated with the constancy of high energy hadronic total cross sections at high energies as in the original Feynman[5] suggestion. The valence quarks are assigned a $dx/\sqrt{x}$ spectrum to account for the presumed Regge behavior and description of the approach to the high energy limit as described by an additional factor of

$\sqrt{x} \propto 1/\sqrt{\nu}$ as $x \to 0$ – i.e., as $\nu \to \infty$, with fixed Q^2. Finally the total amplitude of glue plus sea constituents relative to the valence quarks is fixed by the requirement that $\nu W_2 \propto (1 - x)^3$ for $x \to 1$ in accord with the connection[40] of νW_2 as $x \to 1$ and the asymptotic behavior of the elastic form factor. There remains then but one free parameter, the ratio of numbers of sea quarks to gluons for fitting the neutron and proton scattering data[2] and the massive μ-pair production cross sections,[32] and for predicting spin dependence of the inelastic electron-proton scattering,[41] and the inelastic neutrino-nucleon scattering cross sections.[42] The ratio of longitudinal to transverse cross sections – i.e., the relation between W_1 and W_2 in (25) is fixed by the assumption that the constituents have spin 1/2 and is ab initio in accord with observation. Figures (19), (20), and (21) show the fits to existing data, which in a qualitative sense are satisfactory. The relative contributions of the valence quarks and of the sea and glue is shown in Fig. 19, the fit to which as a function of ω' was accomplished by adjusting the free parameter so that there is twice as much "glue" as "sea." In the absence of glue the calculated curve grows too rapidly for large ω'. The apparent bump in the $\mu\bar{\mu}$ experiment shown in Fig. 21 is not accounted for by this calculation. Most interesting to this approach as noted earlier will be the testing of the scaling law (38), the implications of which for the ISR are shown also in Fig. 21.

The main difficulty with this approach – as with any and all discussions of quarks – is where are they? Why are they not observed? How does one prohibit their appearance short of introducing a strong final state interaction that destroys the simplicity of the parton model? Future experiments that offer a glimpse of what in detail is occurring at the hadronic vertex will add important information and clues to the properties and behavior of the hadron's constituents and their interactions.

A very different approach to this subject is to say that the data is still far from scaling at SLAC energies. Only part of the experimental curve should be fit with partons or light cone behavior, and the rest should be ascribed to remnants of the vector dominance description of photon processes. Suri and Yennie[43] have pursued this line in recent work, suggesting functional forms for fitting the data that are motivated by the behavior (singularities and zeros) resulting from free field commutators. In this way they have made a quantitative fit to the proton data. To them the scaling part accounts for about 70% of the observed νW_2, and the rest is a play between longitudinal and transverse parts that have not yet scaled. From this point of view the light cone region is responsible for the scaling limit but long range contributions within the light cone are still important in analyzing the SLAC-MIT data. These contributions represent the long range hadronic cloud of the photon, and their analysis offers a glimpse at how the approach to scaling may be occurring. The main difference between these approaches lies in the fact that the core quarks and gluons of Kuti and Weisskopf are replaced by the nonscaling long range photon structure in suri and Yennie's approach. They also retain a longitudinal contribution in the asymptotic limit whereas this is ruled out in Kuti and Weisskopf's model by specifying spin 1/2 constituents only.

Another approach to an understanding of the structure functions is based on the observation that the nonvanishing difference between the neutron and proton structure functions implies the existence of a nondiffractive component of virtual photon-proton scattering.[38] Moreover in hadronic reactions such a nondiffractive component at high energies is correlated by the concept of duality with the presence and behavior of resonances at low energy in hadronic reactions. We may apply this concept then also to the electroproduction amplitudes by virtual

photons. This has motivated models[44] with increasing numbers of resonances which add up to the nondiffractive contribution. The problem of harmonizing the notion of partons, or chunks of the nucleon that scatter incoherently and independently of one another, with the notion of resonances, or the collective motions and excitations of the nucleon that scatter coherently, is unresolved at this time.

Perhaps a better distinction between the various models – and according to T. D. Lee[45] a better understanding of the apparently rapid onset of scaling behavior – will come when we get our glimpses of the emerging hadrons in the deep inelastic scattering – and in particular as we get our first views of their multiplicity and how it varies with ω, ν, or Q^2. We have much to learn in the days ahead in this field.

REFERENCES AND FOOTNOTES

1. The newest progress in testing the validity of QED was reviewed in the invited address to this conference by V. Telegdi. See also the contributions by B. Bartali et al. (Paper 257), A. Onuchin et al., and C. Bacci et al.
2. E. D. Bloom et al., Phys. Rev. Letters 23, 930 (1969);
   M. Breidenbach et al., Phys. Rev. Letters 23, 935 (1969);
   G. Miller et al., paper submitted to the XVth International Conference on High Energy Physics, Kiev (1970) (E. D. Bloom et al., SLAC-PUB-796).
3. Such a picture is of course applicable to weakly bound systems such as atoms or even nuclei with packing fractions of no more than 1% or so and is historically successful.
4. For example a neutron bound by an energy that is no more than 0.2% of its mass is stable within a deuterium atom, but β decays in 20 minutes when free.
5. R. Feynman, Phys. Rev. Letters 23, 1415 (1969);
   R. Feynman in Proceedings of the Third Topical Conference on High Energy Collisions of Hadrons, Stony Brook, New York (1969).
6. S. Drell and T. M. Yan, SLAC-PUB-808 (to appear in Ann. Phys. N.Y.).
7. J. Bjorken, Phys. Rev. 148, 1467 (1966).
8. N. Cabibbo, G. Parisi and M. Testa, Lettere Nuovo Cimento 4, 35 (1970).
9. B. Bartali et al., Paper 258, submitted to this conference.
10. C. Bacci et al., cf. Ref. 1.
11. A. Onuchin, paper submitted to this conference.
12. J. Layssac and F. M. Renard, Paper 16 of this conference.
13. F. M. Renard, Nuovo Cimento 64, 979 (1969).

14. G. Kramer, J. L. Uretsky and T. F. Walsh, Phys. Rev. D1, 1617 (1970);
A. M. Altukhov and I. B. Khriplovich, Novosibirsk preprint (1971).

15. A. Bramon and M. Greco, Paper 150 of this conference.

16. S. D. Drell, D. J. Levy and T. M. Yan, Phys. Rev. D1, 1617 (1970).

17. A. Pais and S. B. Treiman, Phys. Rev. 187, 2076 (1969).

18. J. J. Sakurai, Invited paper presented at the Balaton Symposium on Hadron Spectroscopy (1970) (to be published in Acta Phys. Hung.).

19. J. D. Bjorken, private communication.

20. C. F. Cho and J. J. Sakurai, UCLA preprint (April 1971);
P. Longacker and M. Suzuki (to be published);
S. D. Drell and D. J. Silverman, Phys. Rev. Letters 20, 1325 (1968).

21. G. di Giugno et al., Paper 219 of this conference.

22. B. Barish et al., Phys. Rev. Letters 17, 720 (1966);
M. Conversi et al., Nuovo Cimento 40A, 690 (1965).

23. L. Landau and E. Lifshitz, Soviet Phys. 6, 244 (1934);
V. E. Balakin, V. M. Budnev and I. F. Ginzburg, JETP Letters 11, 388 (1970);
S. J. Brodsky, T. Kinoshita and H. Terazawa, Phys. Rev. Letters 25, 972 (1970);
V. N. Baier and V. S. Fadin, Zh. Eksp. Teor. Fiz. 13, 293 (1971);
V. N. Baier and V. S. Fadin, Lettere Nuovo Cimento 1, 481 (1971);
V. N. Baier and V. S. Fadin, Novosibirsk preprint (1971);
S. J. Brodsky, T. Kinoshita and H. Terazawa, CLNS-152 (1971);
N. Arteaga-Romera, A. Jaccarini, P. Kessler and J. Parisi, Phys. Rev. (to appear);
J. Parisi, N. Arteaga-Romera, A. Jaccarini and P. Kessler, PAM 71-Q2 (1971);

Z. Kunszt, R. M. Muradyan and V. M. Ter Antonyan, Dubna preprint E2-5347 (1970);

V. E. Balakin, V. M. Budnev and I. F. Ginzburg, JETP Letters 11, 559 (1970);

A. V. Efremov and I. F. Ginzburg, Dubna preprint E2-5778;

R. W. Brown and I. J. Muzinich, Paper 246 of this conference.

24. H. Cheng and T. T. Wu, Phys. Rev. Letters 24, 1456 (1970).

25. H. Cheng and T. T. Wu, Phys. Rev. Letters 22, 660 (1969).

26. V. G. Serbo, JETP Letters 12, 39 (1970).

27. M. Greco, LNF-7111.

28. D. Benaksos, Paper 347 of this conference.

29. G. Salvini, private communications.

30. J. D. Bjorken, Phys. Rev. 179, 1547 (1969);

R. Jackiw, R. van Royen and G. B. West, Phys. Rev. D2, 2473 (1970);

R. A. Brandt, Phys. Rev. D1, 2808 (1970);

H. Leutwyler and J. Stern, Nucl. Phys. B20, 77 (1970);

B. L. Ioffe, Phys. Letters 30B, 123 (1969);

Y. Frishman, Phys. Rev. Letters 25, 966 (1970).

31. R. L. Jaffe, private communication, to be published.

32. J. H. Cristenson et al., Phys. Rev. Letters 25, 1523 (1970).

33. G. Altarelli, R. A. Brandt, G. Preparata, Phys. Rev. Letters 26, 42 (1971);

A. E. Sanda and M. Suzuki, to be published.

34. S. D. Drell and T. M. Yan, Phys. Rev. Letters 25, 316 (1970) and Ref. 6.

35. R. L. Jaffe, SLAC-PUB-941, to be published.

36. S. J. Brodsky, T. Kinoshita and M. Terazawa, to be published;

T. Walsh, DESY preprint 71/15.

37. D. J. Gross and S. B. Treiman, Paper 345 of this conference;
Y. Frishman et al., Phys. Rev. Letters 26, 798 (1971);
J. Ellis, CERN preprint Th. 1323 (1971).

38. E. Bloom and F. Gilman, Phys. Rev. Letters 25, 1140 (1970).

39. J. Kuti and V. Weisskopf, MIT preprint (May 1971).

40. S. Drell and T. M. Yan, Phys. Rev. Letters 24, 181 (1970);
G. West, Phys. Rev. Letters 24, 1206 (1970).

41. J. Bjorken, Phys. Rev. 148, 1467 (1966); Phys. Rev. D1, 1376 (1970).

42. J. Bjorken and E. Paschos, Phys. Rev. 185, 1975 (1969).

43. A. suri and D. Yennie, SLAC preprint, to be published.

44. P. Landshoff, J. Polkinghorne and R. Short, Nucl. Phys. B28, 225 (1971);
P. Landshoff and J. Polkinghorne, Nucl. Phys. B28, 240 (1971);
P. Landshoff and J. Polkinghorne, Cambridge University preprints (to be published);
G. Domokos, S. Kovesi-Domokos and E. Schonberg, Phys. Rev. D3, 1184, 1191 (1971).

45. T. D. Lee, Columbia University preprint (to be published in Ann. Phys. N.Y.).

FIGURE CAPTIONS

1. Kinematic region for inelastic scattering.
2. SLAC-MIT data for νW_2 plotted as a function of Q^2 for fixed ω=4. For comparison the elastic form factor is plotted on a logarithmic scale along the right-hand ordinate.
3. Proton viewed in the rest frame and in an infinite momentum frame in terms of partons.
4. Data of the Frascati "boson" group plotted as a ratio to the point lepton cross section as a function of E.
5. Mechanism for hadron production via vector meson dominant resonance channels.
6. Kinematic region for annihilation in the process $e\bar{e} \rightarrow$ hadron + anything.
7. Mnemonic for rate of decrease of form factor at large q^2 for the parton as a point quark (Q) the meson as a $(Q\bar{Q})$ and the baryon as a (QQQ).
8. Data on proton form factor from the Frascati $e\bar{e} \rightarrow p\bar{p}$ experiment and comparison with $p\bar{p}$ annihilation measurements and theoretical formulas for a point-like proton and one with a dipole form factor in the time-like region.
9. As in Fig. 8 plotted in terms of the form factor.
10. 2γ contribution to hadron production in ee collisions.
11. Calculations by Brodsky et al. of indicated production channels in the one photon ($e^+e^- \rightarrow \mu^+\mu^-$ and $e^+e^- \rightarrow \pi^+\pi^-$) and two photon equivalent photon mechanisms. Corrections to the point pion approximation are also indicated in the σ curve.
12. Noncoplanarity in $\pi^+\pi^-$ production viewed end on which the colliding e^+e^- beams.

13. Region near the light cone contributing to deep inelastic electron scattering.

14. Massive pair formation by parton-antiparton annihilation in a p-p collision.

15. Feynman diagram for massive pair production in perturbation theory. Scaling results when both the intermediate lines are near the mass shell.

16. Massive pair production in γp collision by (a) partons and (b) Bethe-Heitler mechansim.

17. Calculation of massive muon pair formation by photons with a bremsstrahlung spectrum with a 7 GeV peak.

18. Deep inelastic scattering from a "photon" in an $e\bar{e}$ collision.

19. Fit to νW_2 in the Kuti-Weisskopf model. The dashed curve represents the contribution of the valence quarks and the dot-dashed one, that of the sea plus glue.

20. Kuti-Weisskopf fit to the neutron-proton difference.

21. Kuti-Weisskopf fit to process (33) for massive lepton pair production. The solid line uses the parameters applied in Figs. 19 and 20. The dashed line is for no glue present. The dotted and dot-dashed curve are predictions for the ISR based on the scaling law (38).

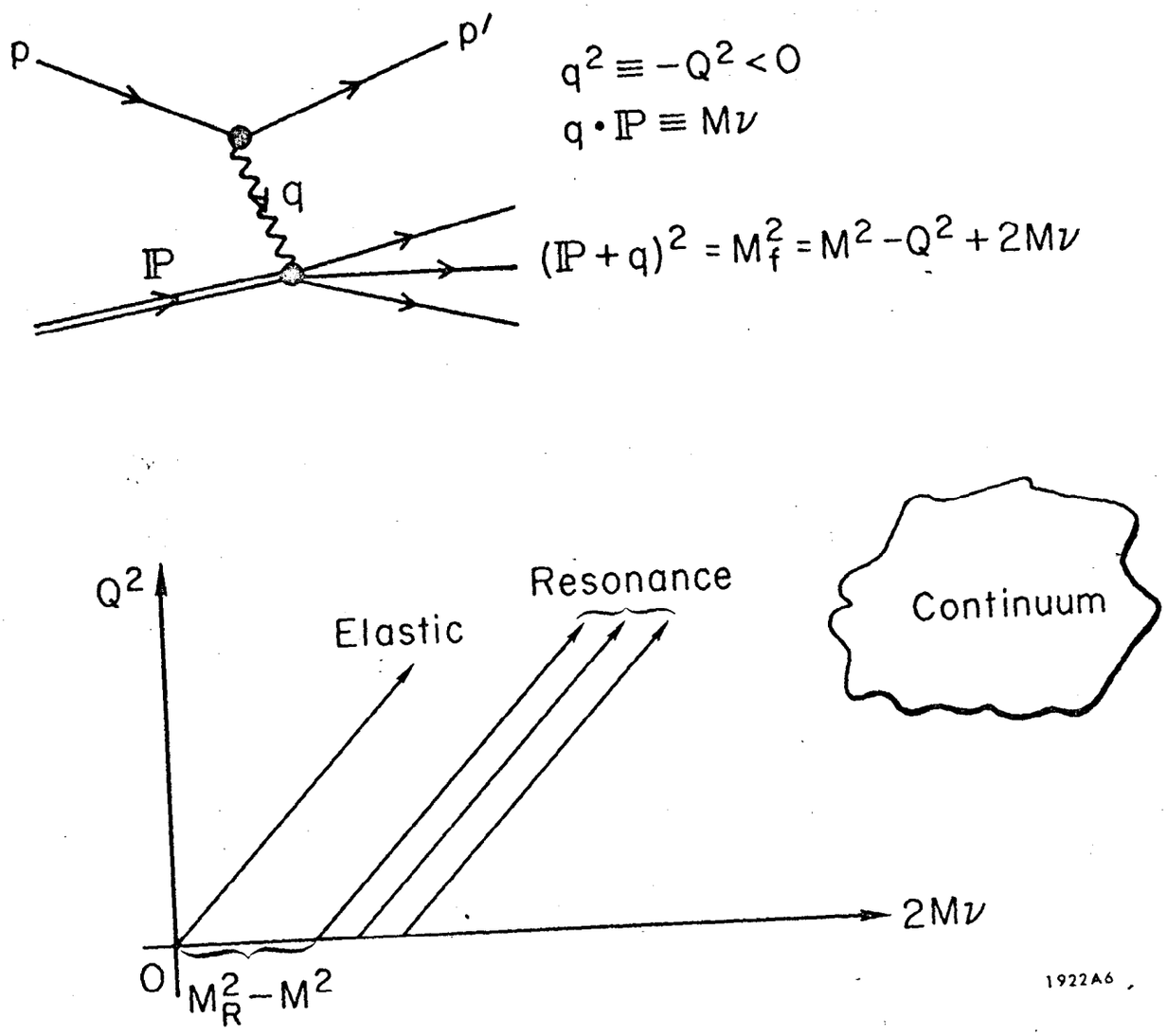
p
p′
q
IP
$q^2 \equiv -Q^2 < 0$
$q \cdot IP \equiv M\nu$
$(IP+q)^2 = M_f^2 = M^2 - Q^2 + 2M\nu$
Q^2
Elastic
Resonance
Continuum
$2M\nu$
O
$M_R^2 - M^2$
1922A6

Fig. 1

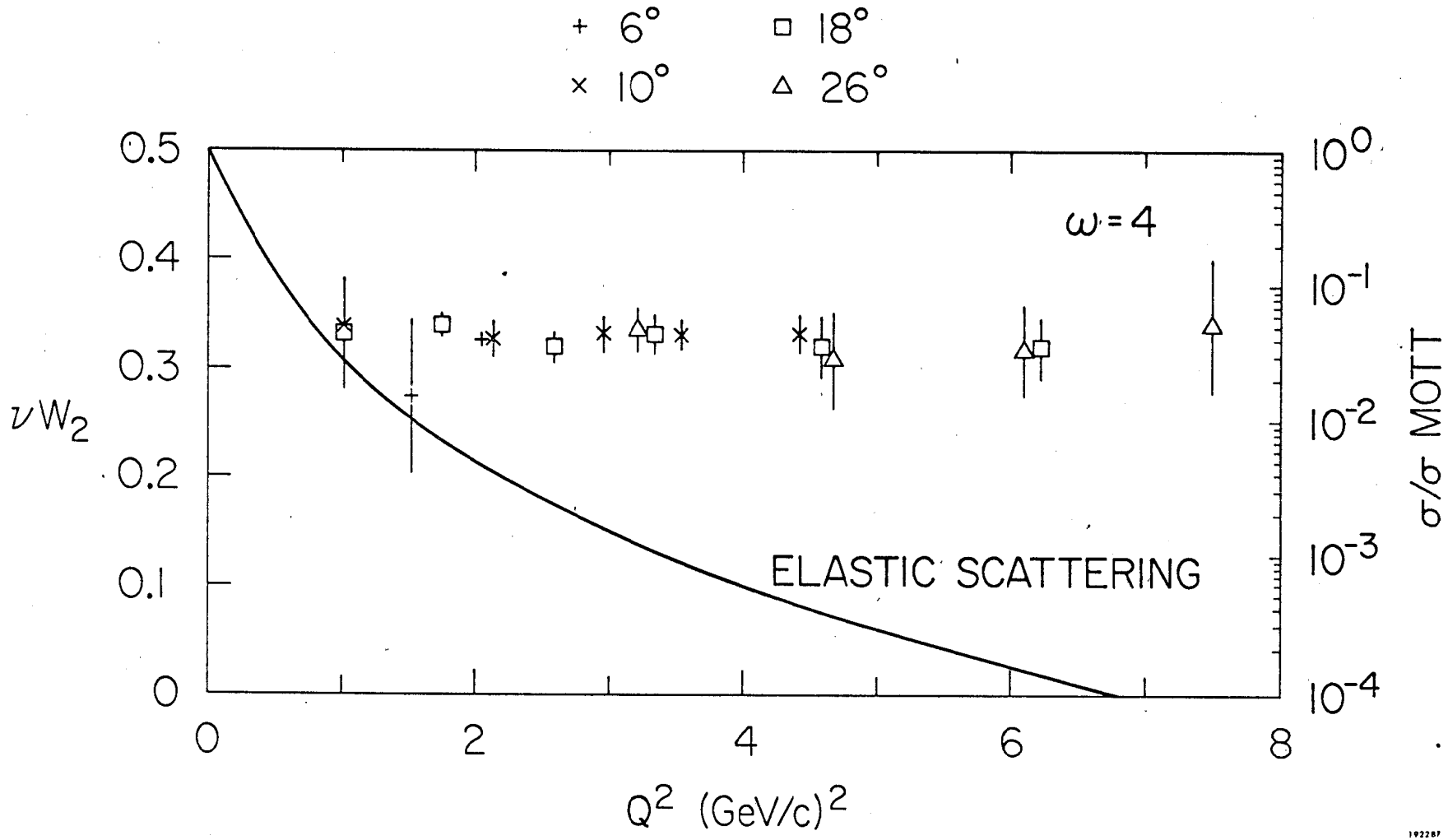
+ 6°
□ 18°
× 10°
△ 26°
0.5
0.4
0.3
0.2
0.1
0
νW_2
$\omega = 4$
ELASTIC SCATTERING
10^0
10^{-1}
10^{-2}
10^{-3}
10^{-4}
σ/σ MOTT
0
2
4
6
8
Q^2 (GeV/c)^2
192287

Fig. 2

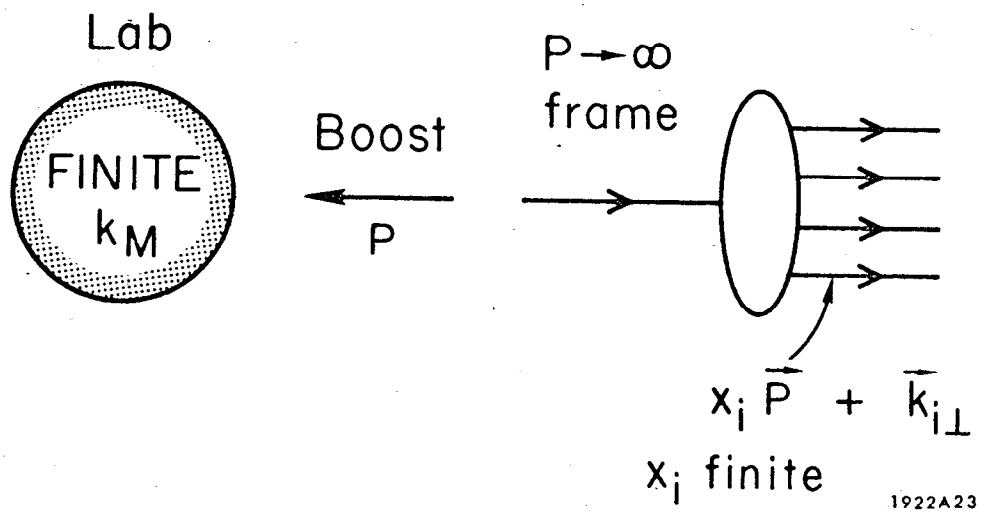
Lab
FINITE
k_M
Boost
P
$P \to \infty$
frame
$x_i \vec{P} + \vec{k}_{i\perp}$
x_i finite
1922A23

Fig. 3

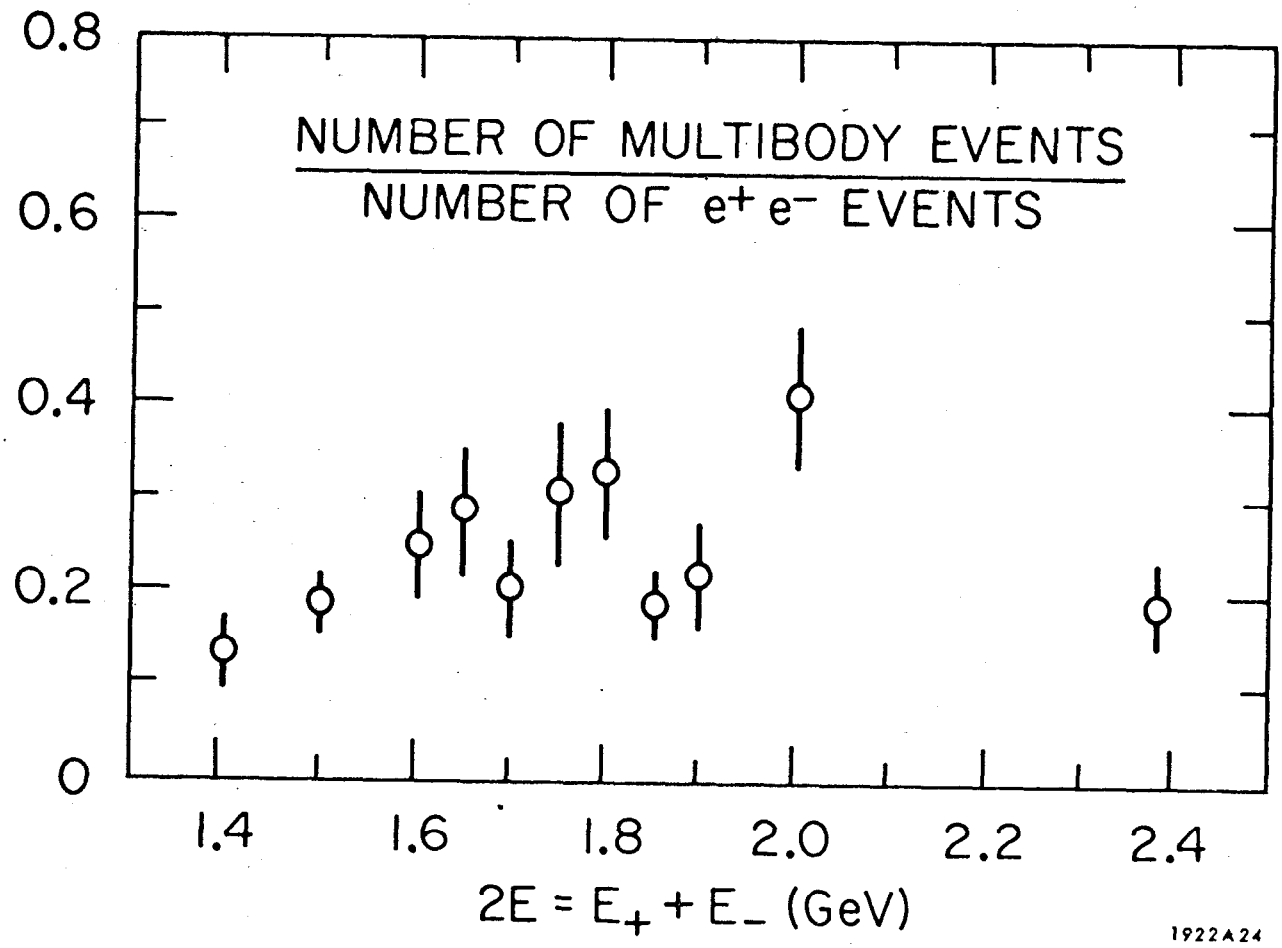
0.8
0.6
0.4
0.2
0
NUMBER OF MULTIBODY EVENTS
NUMBER OF e+ e− EVENTS
1.4
1.6
1.8
2.0
2.2
2.4
2E = E+ + E− (GeV)
1922A24

Fig. 4

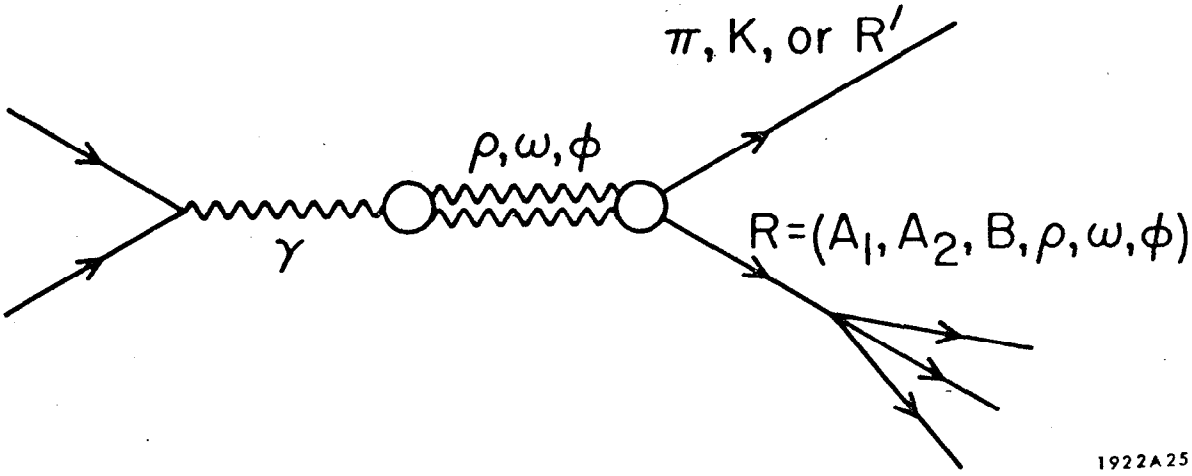

Fig. 5

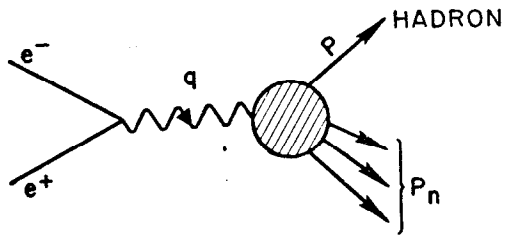

$e\bar{e} \longrightarrow h + \text{ANYTHING}$

1353A2

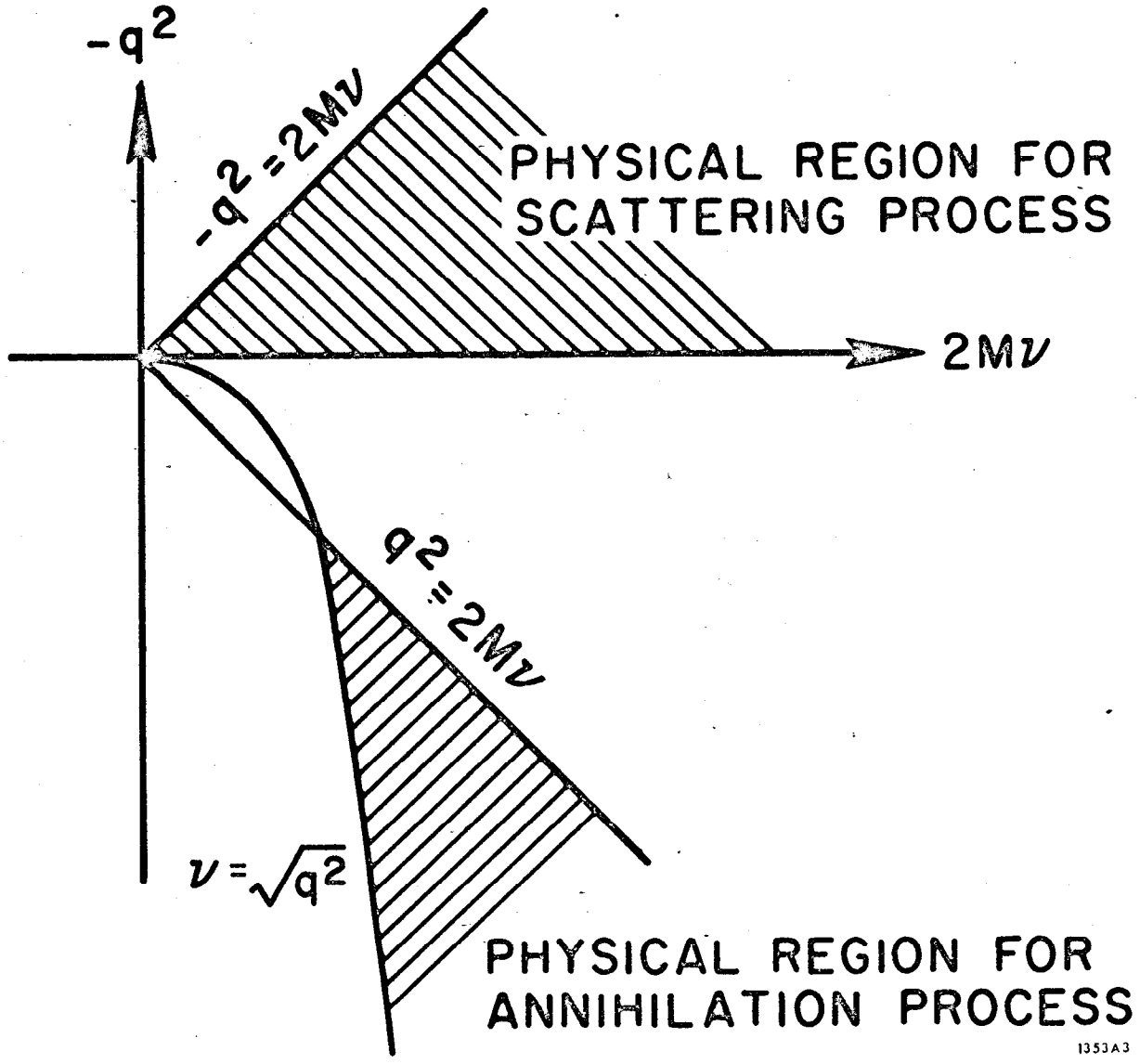

1353A3

Fig. 6

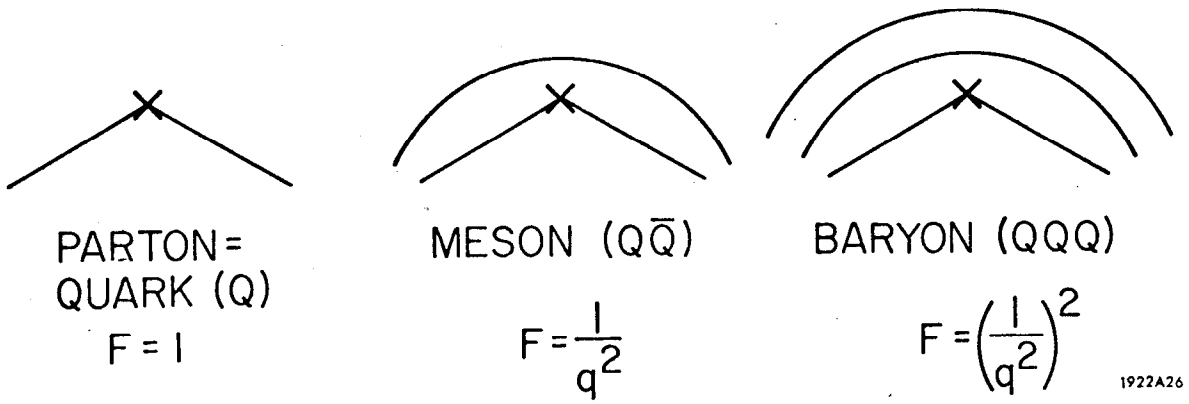

Fig. 7

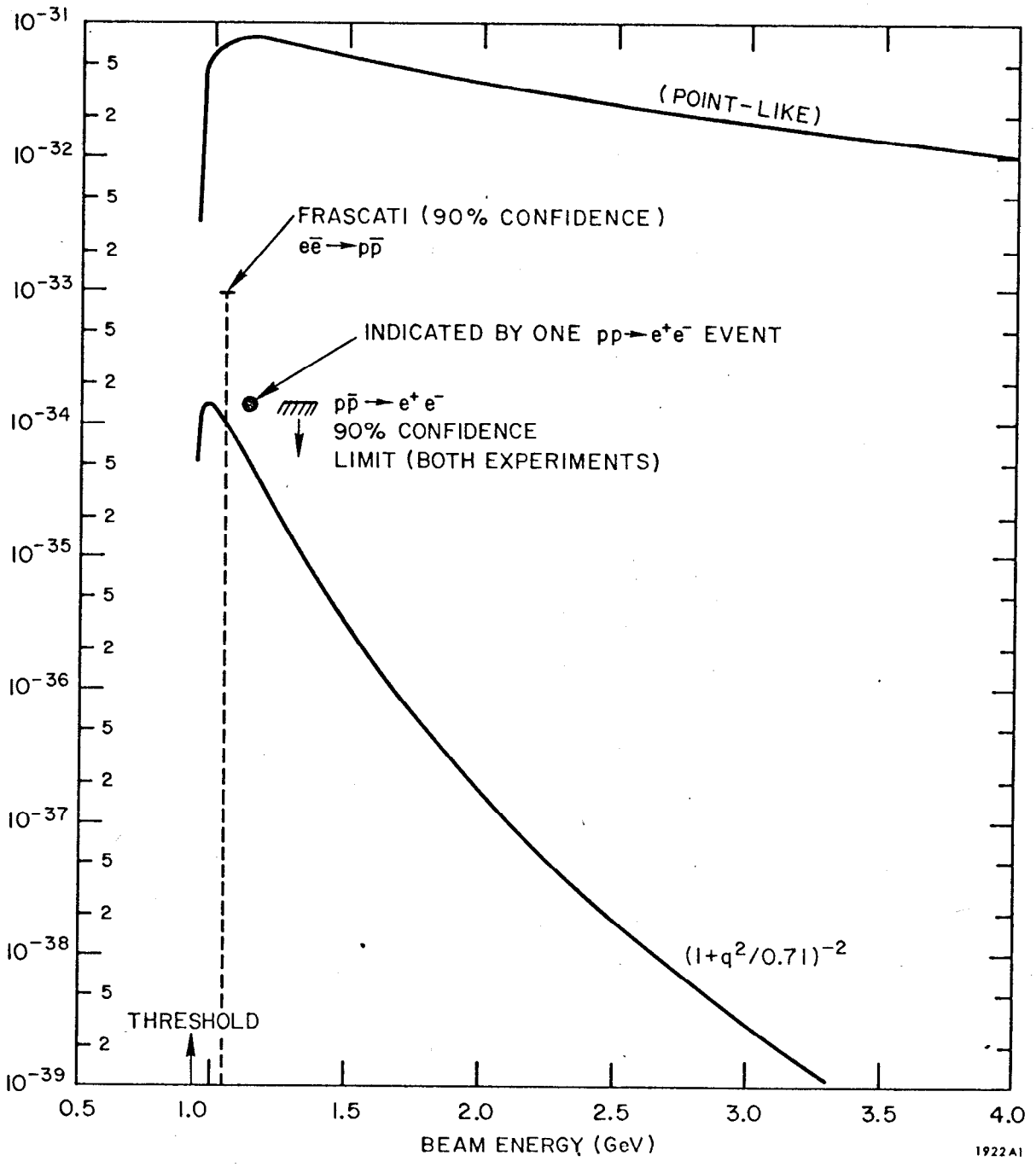
(POINT-LIKE)
FRASCATI (90% CONFIDENCE)
$e\bar{e} \rightarrow p\bar{p}$
INDICATED BY ONE $pp \rightarrow e^+e^-$ EVENT
$p\bar{p} \rightarrow e^+e^-$
90% CONFIDENCE
LIMIT (BOTH EXPERIMENTS)
$(1+q^2/0.71)^{-2}$
THRESHOLD
10^{-31}
10^{-32}
10^{-33}
10^{-34}
10^{-35}
10^{-36}
10^{-37}
10^{-38}
10^{-39}
5
2
0.5
1.0
1.5
2.0
2.5
3.0
3.5
4.0
BEAM ENERGY (GeV)
1922A1

Fig. 8

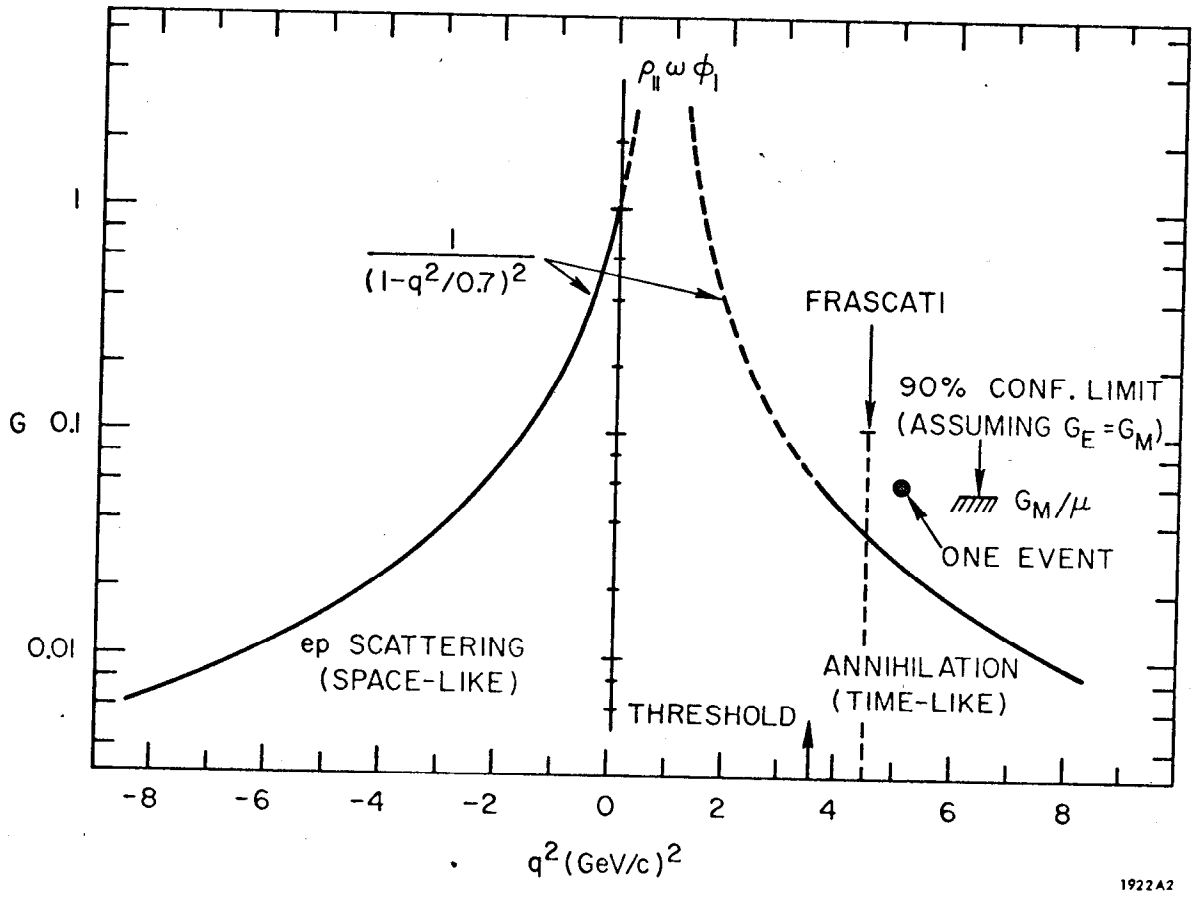
$\rho_{II}\,\omega\,\phi_I$
1
G 0.1
0.01
$\frac{1}{(1-q^2/0.7)^2}$
FRASCATI
90% CONF. LIMIT
(ASSUMING $G_E = G_M$)
G_M/μ
ONE EVENT
ep SCATTERING
(SPACE-LIKE)
ANNIHILATION
(TIME-LIKE)
THRESHOLD
-8
-6
-4
-2
0
2
4
6
8
q^2(GeV/c)^2
1922A2

Fig. 9

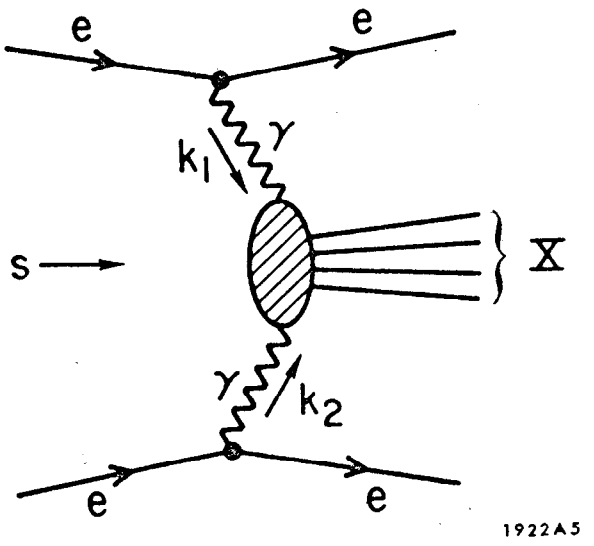

Fig. 10

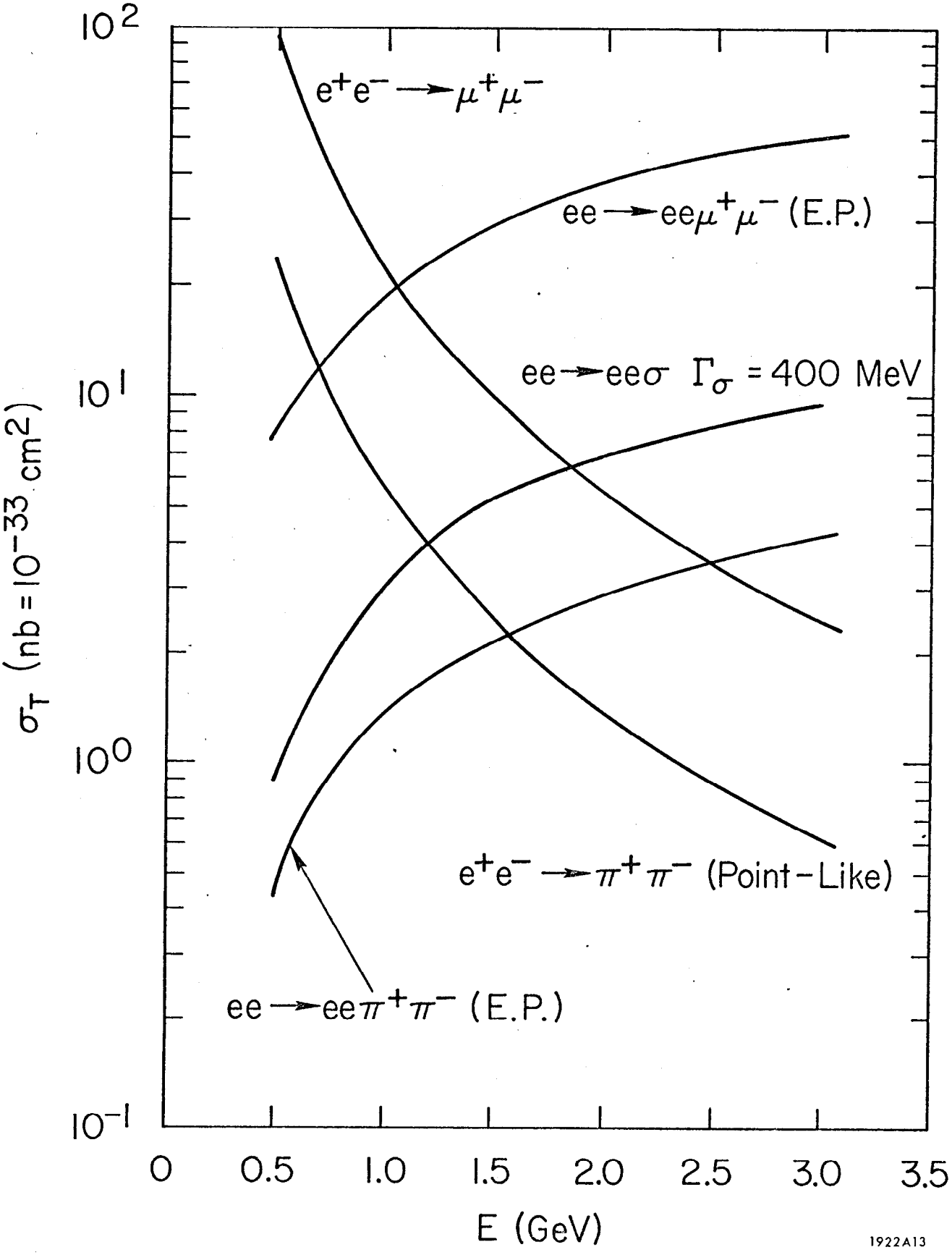
10^2
10^1
10^0
10^{-1}
σ_T (nb = 10^{-33} cm^2)
$e^+e^- \rightarrow \mu^+\mu^-$
$ee \rightarrow ee\mu^+\mu^-$ (E.P.)
$ee \rightarrow ee\sigma$ Γ_σ = 400 MeV
$e^+e^- \rightarrow \pi^+\pi^-$ (Point-Like)
$ee \rightarrow ee\pi^+\pi^-$ (E.P.)
0
0.5
1.0
1.5
2.0
2.5
3.0
3.5
E (GeV)
1922A13

Fig. 11

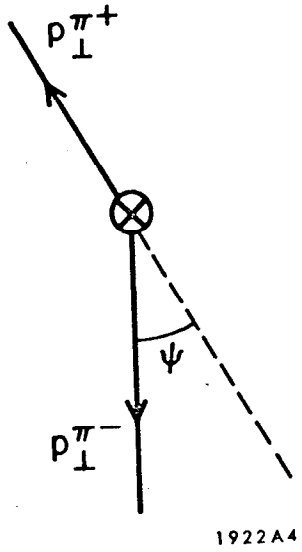

Fig. 12

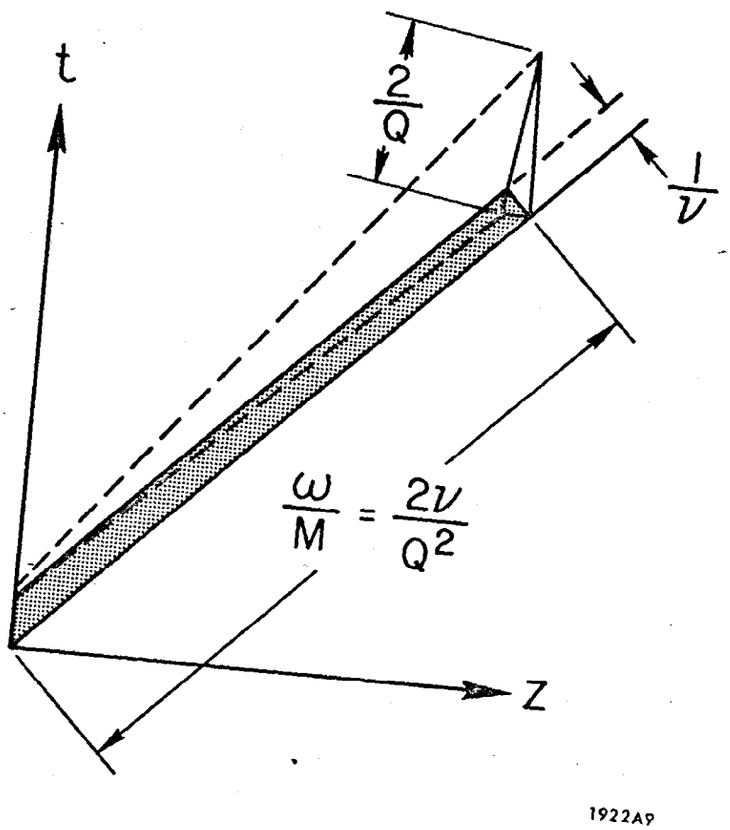

Fig. 13

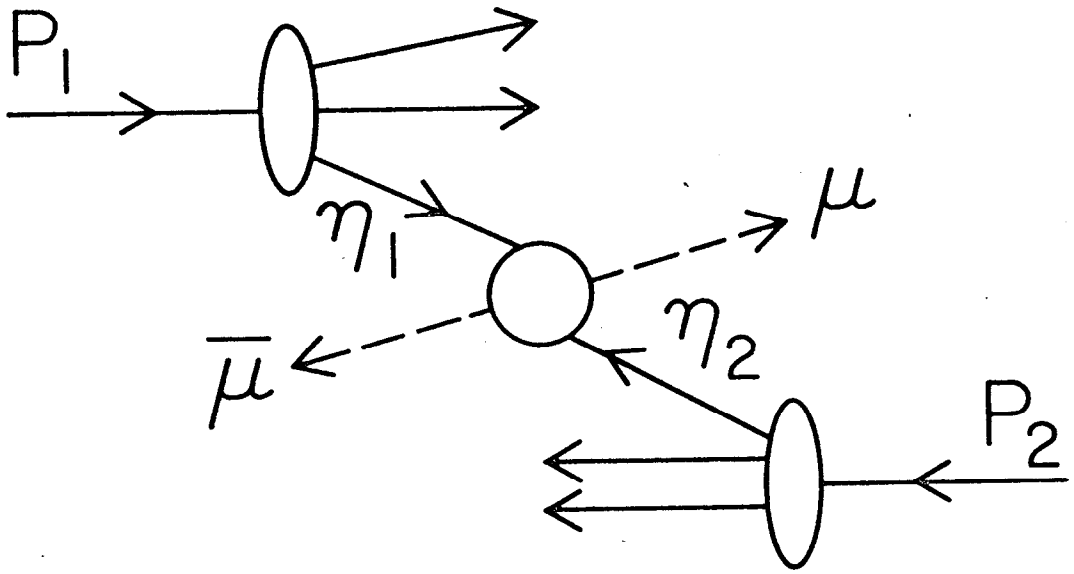

$$Q^2 = \eta_1 \eta_2 S$$

1589A3

Fig. 14

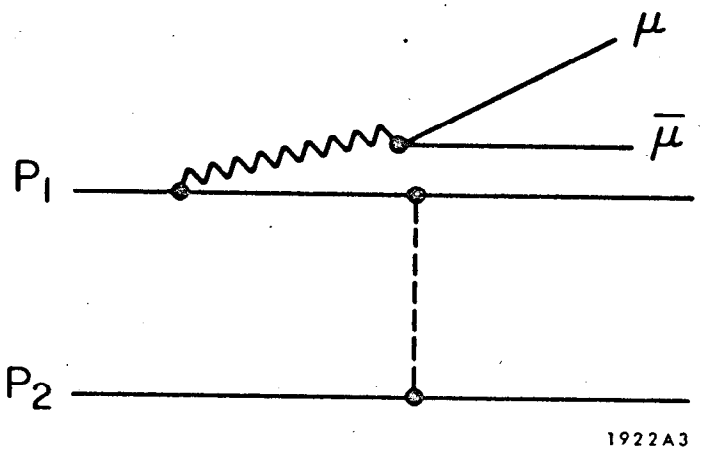

Fig. 15

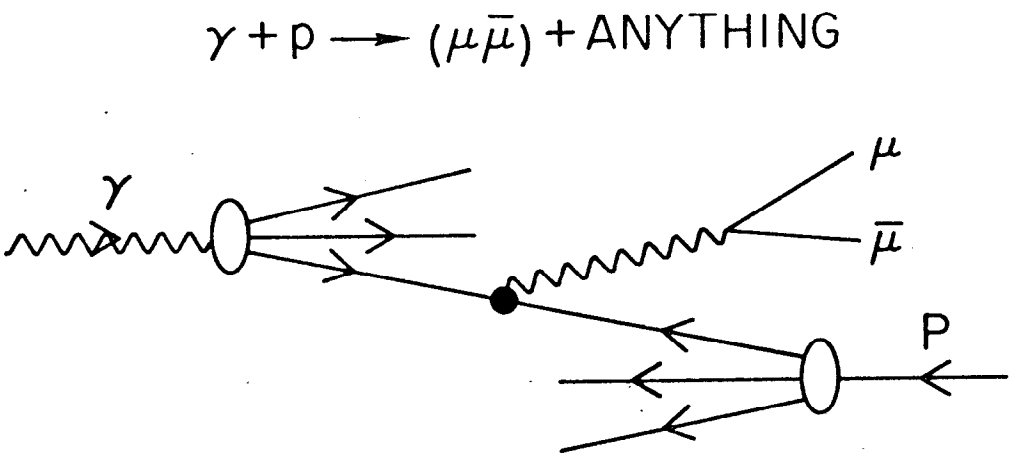

(a) PARTON

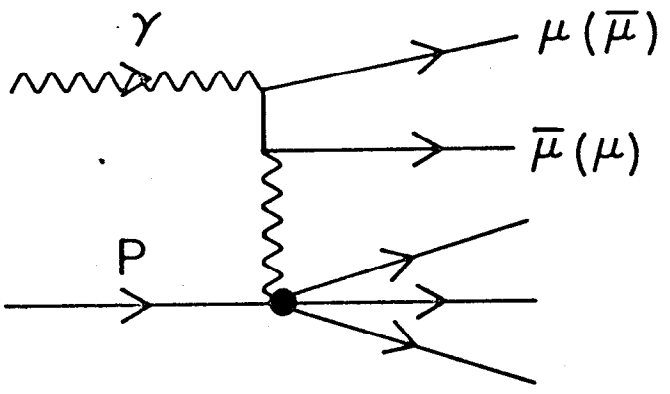

(b) BETHE–HEITLER

1922A14

Fig. 16

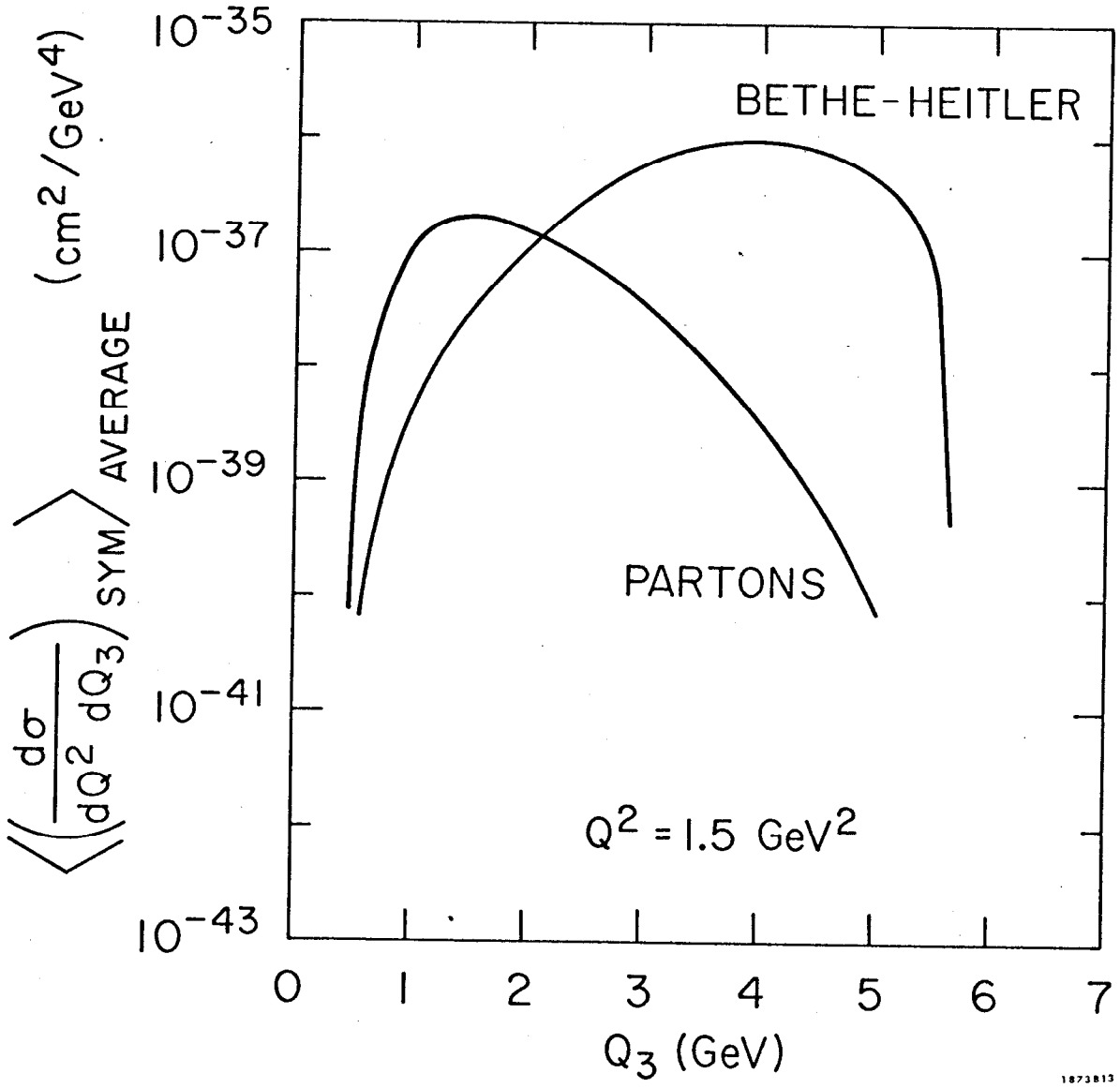
10^{-35}
10^{-37}
10^{-39}
10^{-41}
10^{-43}
$\left\langle \left(\frac{d\sigma}{dQ^2\, dQ_3} \right)_{SYM} \right\rangle_{AVERAGE}$ (cm^2/GeV^4)
BETHE-HEITLER
PARTONS
$Q^2 = 1.5\ GeV^2$
0 1 2 3 4 5 6 7
Q_3 (GeV)
1873B13

Fig. 17

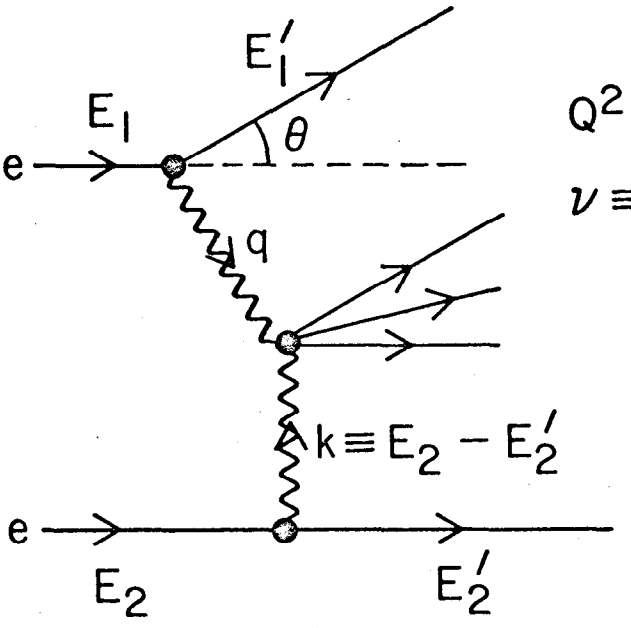

$$Q^2 = 4E_1 E_1' \sin^2 \frac{\theta}{2}$$

$$\nu \equiv q \cdot k = 2k\left(E_1 - E_1' \cos^2 \frac{\theta}{2}\right)$$

1922A15

Fig. 18

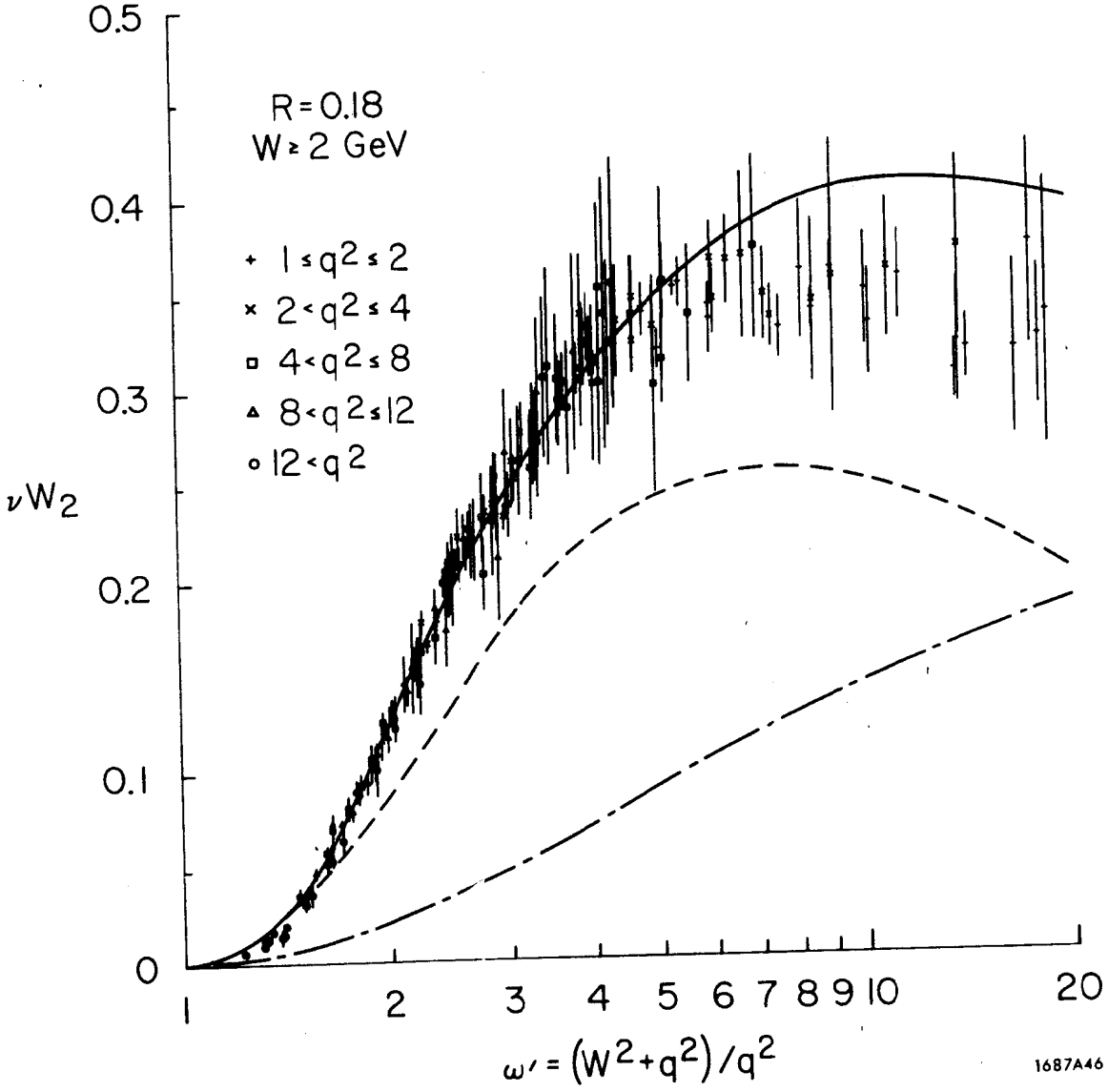
0.5
0.4
0.3
0.2
0.1
0
R=0.18
W≥2 GeV
+ 1≤q²≤2
× 2<q²≤4
□ 4<q²≤8
△ 8<q²≤12
○ 12<q²
νW2
1
2
3
4
5
6
7
8
9
10
20
ω' = (W²+q²)/q²
1687A46

Fig 19

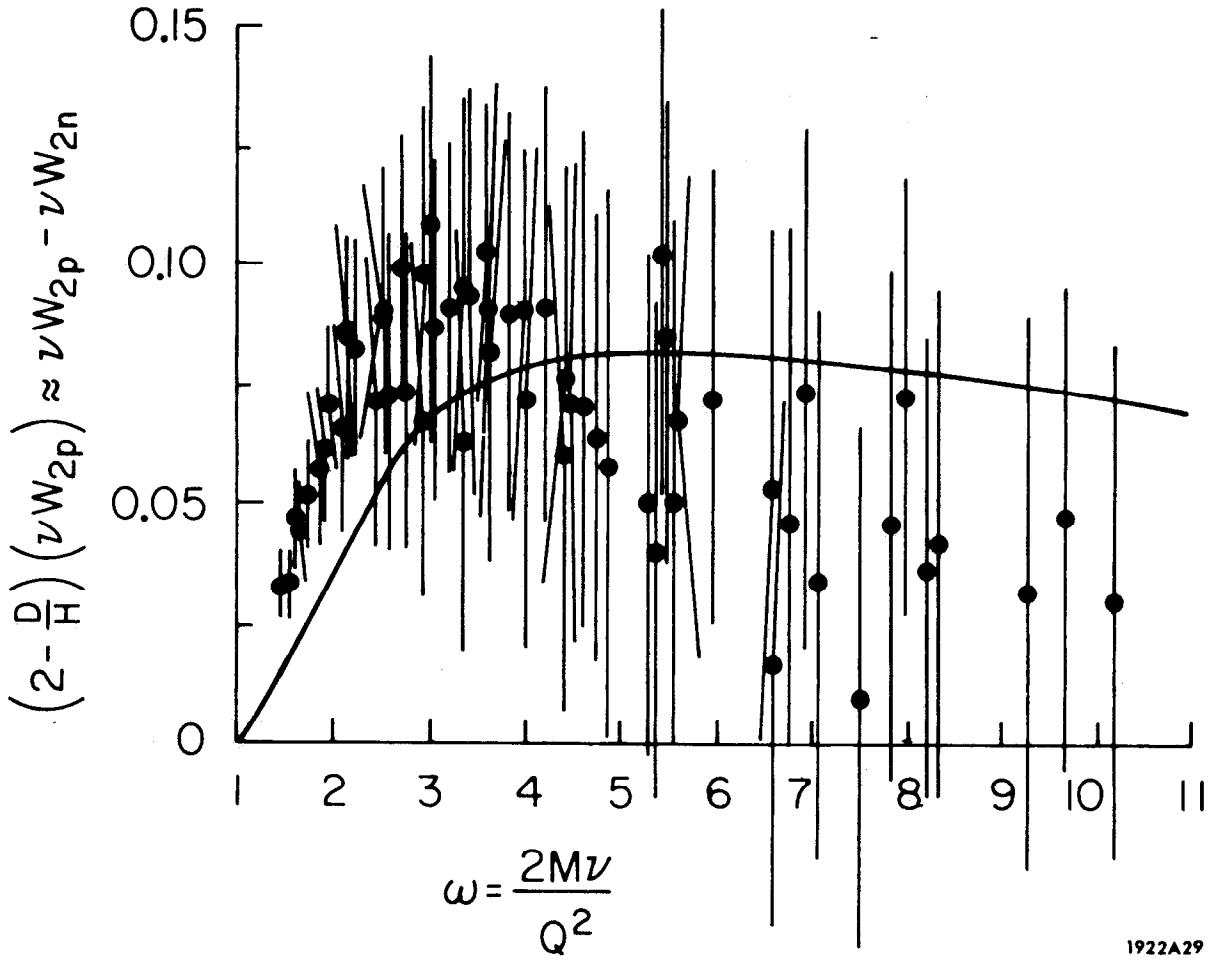
0.15
0.10
0.05
0
1
2
3
4
5
6
7
8
9
10
11
$\left(2-\frac{D}{H}\right)\left(\nu W_{2p}\right) \approx \nu W_{2p} - \nu W_{2n}$
$\omega = \frac{2M\nu}{Q^2}$
1922A29

Fig. 20

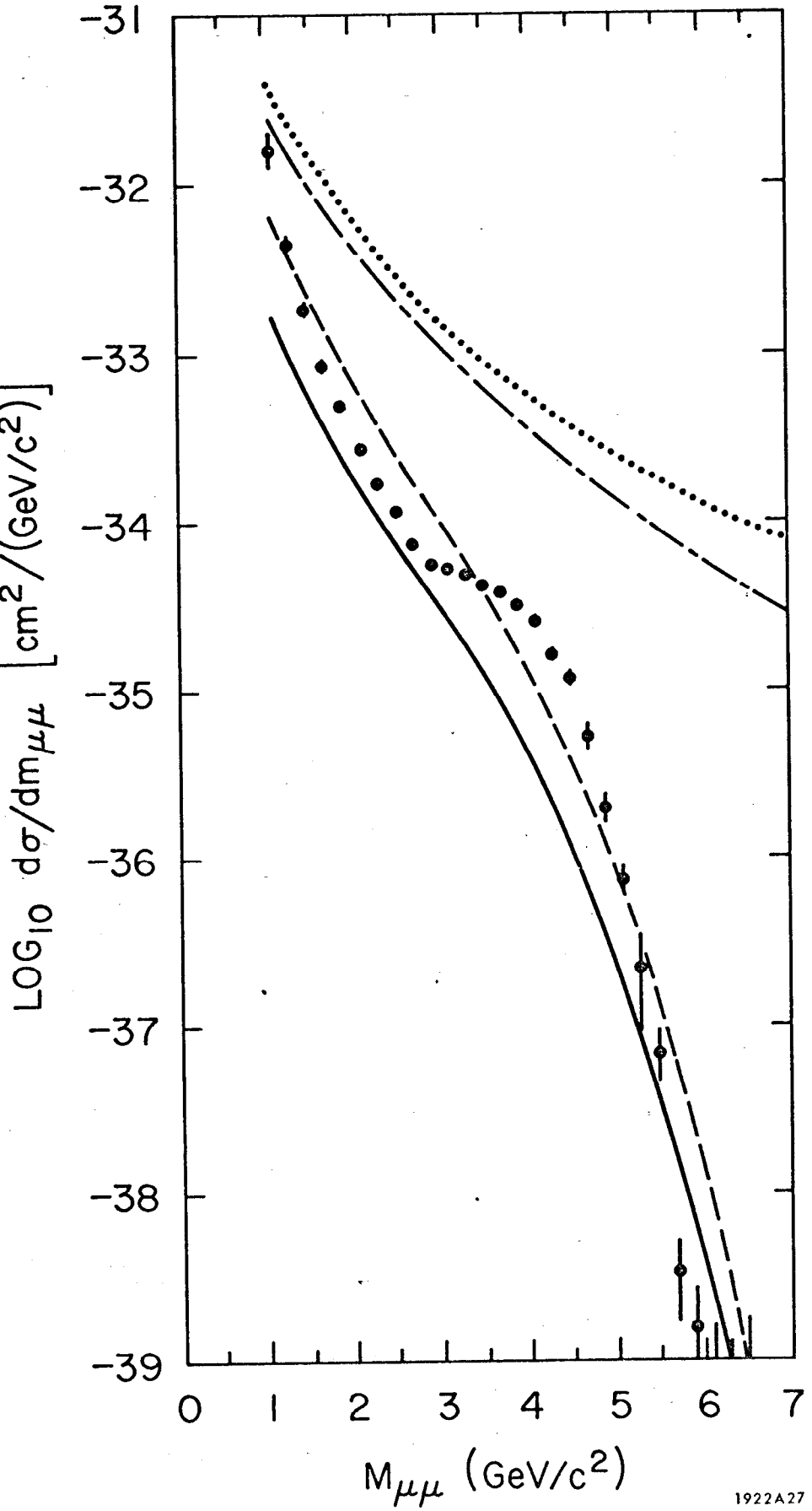
-31
-32
-33
-34
-35
-36
-37
-38
-39
0
1
2
3
4
5
6
7
LOG10 dσ/dmμμ [cm2/(GeV/c2)]
Mμμ (GeV/c2)
1922A27

Fig. 21